Operation of Horizontal Axis Wind Turbines in Arrays

A dissertation submitted to the University of Manchester for the degree of Master of Science in the Faculty of Engineering and Physical Sciences

2018

Fengnan Sun

School of Electrical and Electronic Engineering

Contents

List of Figures

List of Tables

Nomenclature

Notation	Meanings	Unit
A	Area of the rotor sweeping area	m^2
a	Induction factor	
C_P	Power coefficient	
C_T	Thrust coefficient	
c_1	A constant denoting the non-dimensional length	
D	Rotor diameter	m
D_{eff}	Efficient rotor diameter	m
D_{wake}	The diameter of wake	m/s
h	Hub height	m
I_a	Ambient turbulence intensity	
I_w	Mechanical generated turbulence intensity	
k	Wake decay constant	
r	Radial distance	m
$R_{9.5}$	Represents the wake radius at a distance of 9.5D downstream form the turbine	m
s	Axial distance (normalized by D)	
U_0	The equivalent onset wind speed for the turbine	m/s
ΔU	The velocity deficit	m/s
x_0	A constant representing the downstream turbine's position	m
x	Distance between upstream and downstream turbine	m
z_0	Roughness length	
β	Wake expansion parameter	

Abstract

The wake effect caused by wind turbines can induce significant velocity deficit and increase the mechanical turbulence intensity that influence the velocity field within a wind farm. As long as the velocity field changes, the power output and loading of each turbine within the wind farm will change.

As a result, the wake effect is a crucial factor that affect the overall performance of a wind farm. To study the wake effect, two kinds of models were developed and widely used in existing research: computational wake models (CFD simulation) and analytical wake models (kinematic wake models). The CFD is accurate but very expensive. Therefore, the four analytical wake models (Jensen, Larsen, Frandsen and Ishihara wake models), that are more simplified and cheap wake simulation methods, have been tested and evaluated first by comparing with CFD simulation results in this thesis.

Then, three commonly used wake combination methods in analytical wake models has been tested and evaluated in the similar way.

Larsen wake model and Linear wake combination method have been chosen as the most appropriate methods to do the further power output simulation for typical two-turbines array (inline or partly-offset) and typical four-turbines array unit based on the study mentioned above. From the power output simulation and energy simulation results, it can be found that using the adjusted C_T operation strategy can increase the energy yield by 0.164% of the total energy yield for the 4-turbines array unit. On the other hand, the adjusted C_T operation strategy can slightly improve the stability of total power output for this array.

Declaration

I declared that the thesis is written by myself solely, and all the places that have referred to methods, results or conclusions of previous researches have been marked with the source of the literature. All the MATLAB programs to develop four wake models and other relative research work have been completed by myself. This thesis has not been submitted by any other student for any kind of degrees before.

Intellectual Property Statement

The intellectual property rights statement in this thesis is as follows:

(explanation: IP statement is an obligatory part as claimed in the MSc project handbook 2017-2018 and the following text is the same with almost all other MSc project theses of The University of Manchester)

i. The writer of this thesis owns the copyright or any other intellectual property right in it and she has given the rights to The University of Manchester to use it.

ii. "Copies of this dissertation, either in full or in extracts and whether in hard or electronic copy, may be made only in accordance with the Copyright, Designs and Patents Act 1988 (as amended) and regulations issued under it or, where appropriate, in accordance with licensing agreements which the University has entered into. This page must form part of any such copies made."

iii. "The ownership of certain Copyright, patents, designs, trademarks and other intellectual property (the "Intellectual Property") and any reproductions of copyright works in the dissertation, for example graphs and tables ("Reproductions"), which may be described in this dissertation, may not be owned by the author and may be owned by third parties. Such Intellectual Property and Reproductions cannot and must not be made available for use without the prior written permission of the owner(s) of the relevant Intellectual Property and/or Reproductions."

iv. "Further information on the conditions under which disclosure, publication and commercialisation of this dissertation, the Copyright and any Intellectual Property and/or Reproductions described in it may take place is available in the University IP Policy (see documents.manchester.ac.uk/display.aspx?DocID=487), and any relevant Dissertation restriction declarations deposited in the University Library, The University Library's regulations (see manchester.ac.uk/library/aboutus/regulations) and in The University's Guidance for the Presentation of Dissertations."

Acknowledgements

I would like to express my gratitude to my supervisor Dr. Timothy Stallard and his student Dr. Christoph Hachmann first. My supervisor Dr. Stallard met me very frequently to answer all my questions with great patience and to give me very constructive suggestions for each step in my dissertation. He not only taught me professional knowledge, but also encouraged me a lot, especially when I was not confident to do the programming job by my own. Dr. Hachmann also helped me a lot in this dissertation project, especially in terms of details, like dealing with wind data.

I would like to thank all my friends who helped me a lot in MATLAB programming, like Xiaoyu Chen, Xiaoqing Chen, Yue Cheng etc. They are all every excellent student in different engineering areas. Because this is the first time that I use MATLAB to do a project alone, their advice on programming helped me a lot at the very beginning.

I would like to thank my dear parents, who have been supporting me throughout my entire life. They tried their best to give me good education and a lovely family. I will be grateful forever to my mother and father.

1 Introduction

1.1 Background and Motivation

The industry of wind energy has been developing rapidly since 2005 and reached a global wind power installation of 433 GW by the end of 2015 (Global Wind Energy Council, 2017). Especially in countries that have relatively abundant wind source and high energy demand that create advantageous condition for wind power industry like United States, China, Germany, United Kingdom and India, the industry growth rate is rather prodigious. As figure 1 shows, the scenario of wind energy is also quite promising that has been predicted to account for 13% of the whole energy supply in 2040.

For such a valuable and profitable industry, in order to make wind energy more reliable and cheaper, it is still very challenging and beneficial in investigating the characteristics of flow-field and setting more reasonable operation strategies, maximizing the efficiency and stability of power output for a specific wind farm.

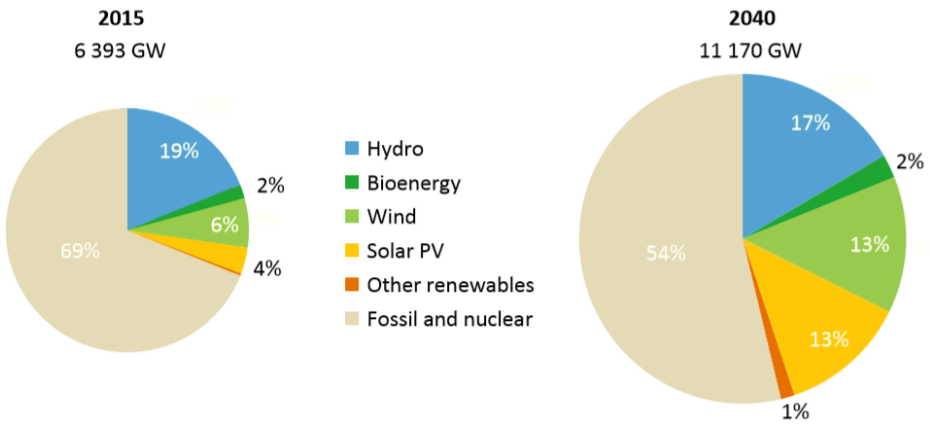

Fig. 1 Scenario of world power generation by energy source by 2040

(International Energy Agency, 2016)

The flow-field that develops through a wind farm flow directly influences the power output and loading of each turbine within the array. Principle operating parameters for each turbine include the tip-speed-ratio, power coefficient and thrust coefficient and yaw angle, and each in-turn influence the downstream flow and hence performance of the array as a whole. For a specific configuration of turbines, it is desirable to operate the array to achieve a number of alternative objectives. For low flow speeds, optimization of power supply is typically required. Alternatively, a

target rate of change of power is desirable to facilitate network integration and standardization of load cycles per turbine desirable to maximize design life of individual components.

Considerable progress in the fundamental analysis of flow within arrays has been achieved through detailed CFD computations and physical experiment at various scales. However, such methods are expensive and simplified approaches to modeling arrays are required to evaluate alternative control strategies for the arrays over intervals of months or years (Crasto, Gravdahl, Castellani, & Piccioni, 2012). For this purpose, simplified semi-empirical wake models, and wake-combination methods, are widely used in practice.

This project will develop and investigate a simple approach to modeling the wake-field within, and downstream of an array to assess the influence of turbine specific operating parameters on the power output and wake of an array as a whole.

1.2 Problem Analysis

The main problem is to quantify the wake effect in a specific wind farm to map the flow velocity field under different onset wind and operation strategies. As the airfoils of wind turbines rotate in an air flow field, kinetic energy of flowing air will be extracted and transformed into mechanical energy of wind turbine, which will be the impetus of electric generators. The wind speed will decrease suddenly as wind flows across the turbine, and the turbulence intensity will increase at the same time. In the ideal case, these two indices will recover to the initial value of the onset wind, but in real situation, with spacing between the turbines ranged from only 4D to 8D (rotor diameter) in offshore wind farms, turbines downstream are still exposed to the negative influence of deficit wind speed and increased turbulence intensity, generating less electricity compared to turbines upstream (Son, Lee, Hwang, & Lee, 2014). That is why the distance designing between turbines is quite crucial for increasing the energy yield (Choi, Hyun Nam, Hyun Jeong, & Chun Kim, 2013).

The wind turbines wakes can be influential enough to cause power losses as high as 15% of the total power output from a wind farm (Barthebnie et al., 2004). As a result, it is quite essential to establish an accurate flow velocity field based on wake analysis to forecast the energy yield of a

wind farm regarding to the mutual interaction between turbines (N. Moskalenko, Rudion, & Orths, 2010a).

1.3 Objectives and Methodology

The aim of this project is to further develop semi-empirical wake models to account for the influence of key turbine operating parameters – such as tip-speed-ratio, power coefficient, thrust coefficient and yaw (Miao, Li, Pavesi, Yang, & Xie, 2017)– and employ this approach to assess the influence of turbine specific operating parameters on the power output and wake of an array as a whole. This will be accomplished by:

- Review of wind-turbine wake parameterization models to establish dependency of wake structure on thrust coefficient and environmental conditions.
- Identification of modification of wake-models to account for turbine operating parameters such as yaw and power coefficient.
- Collate CFD or experimental datasets to compare with analytical wake model simulation results.
- Employ appropriate array wake models to predict power output for a case study array using resource data for a typical site.
- Evaluate the influence of turbine operating strategies on the time-varying power from the array for the objective of maximum energy generation.

1.4 Thesis Outline

Chapter 2 will summarize the four analytical wake models in the existing literature firstly, including their basic principles and the formulas needed for modeling. Then, single wake test will be made and be compared with CFD single wake simulation results to decide which model is the best in depicting the velocity field after a single turbine.

In chapter 3, three commonly used wake combination methods referred to as Largest Deficit, Linear and Root-Sum-Square will be tested when two turbines are inline, partly-offset and fully-offset. The simulation results will be compared with corresponding CFD simulation results to decide which wake combination method is the most accurate one.

In these two chapters, all analytical models adopt the same parameters as the benchmark because published CFD results.

Chapter 4 will discuss the effect of operation strategies on power generation under different conditions (the position of two turbines, different U_0, pitch control). One strategy is that both of the turbines are in their optimal performance according to the onset wind velocity. The other one is to alter the C_T of the upstream turbine in order to get the maximum total power output.

Chapter 5 will calculate the total power output for 4-turbines array unit according to real wind data of 8760 hours under two different operation strategies and evaluate the potential value of altering operation strategies of horizontal axis wind turbines in arrays.

The last chapter will give conclusions of this dissertation project and provide Recommendations for the future work.

2 Literature Review

Turbine wake models are classified into five categories, as table 1 shows.

Table 1 Classification of wake models-this table is from (B.Sanderse, 2011)

Method	Blade model	Wake model
Kinematic	Thrust coefficient	Self-similar solution
BEM	Actuator disk+ blade element	Quasi one-dimensional momentum theory
Vortex lattice, vortex particle	Lifting line/surface+ blade element	Free/fixed vorticity sheet, particles
Panels	Surface mesh	free/fixed vorticity sheet
Generalized actuator	Actuator disk/line/surface	Volume mesh, Euler/RANS/LES
Direct	Volume mesh	Volume mesh, Euler/RANS/LES

Two types of wake models are considered in this study. One type is referred to as analytical wake model (the kinematic method) and this is the main object of study. Such tools are widely used evaluate energy yield for specific array layouts (B.Sanderse, 2011). The other type is named as computational wake model. Such approaches can describe the flow very accurately and published results from this type of simulation will be used as benchmark to verify implementation of alternative analytical wake models (Tong, Chowdhury, Zhang, & Messac, 2012). Because computational wake models commonly use Computational Fluid Dynamics (to solve the Navier-Stokes equations), it is called as CFD model hereinafter.

2.1 Single Wake Models

As mentioned in the section 1.3, four simple wake models (Jensen, Larsen, Frandsen and Ishihara Model) were chosen to be tested. These four models are all kinematic models. Unlike field models which are based on Navier-Stokes or vorticity transport equations (González-Longatt, Wall, & Terzija, 2012), kinematic models are developed only based on momentum equation and require less computation. In this chapter, a short overview of these four wake models will be presented, all equations refer to the existing literature (Tong et al., 2012), all parameters are verified according to literature study and four single wake models (under offshore environment) will be established respectively and compared with each other.

In order to reflect the difference between velocity fields established by four models, the same colored scale, having the speed range from 0.1 to 1.0 or from 0.5 to 1.0 (normalized velocity according to onset wind velocity), has been used both longitudinal and transverse profiles.

2.2 Jensen Model

Proposed by N.O.Jensen (Jensen, 1983) and developd by Katic, as one of the oldest wake model, Jensen model has been applied widely in the wind power industry because of its simple function relationship. The Jensen model provides a relationship for the far wake only and neglects the near wake in order to simply the model equation, which can overestimate the power losses (Sun & Yang, 2018b). However, it is still a consistent and reliable wake model for large scale wind farms energy estimation (Tian, Zhu, Shen, Song, & Zhao, 2017).

The diameter of the wake is only dependent on the wake decay constant k and the axial distance downstream s (respect to the rotor diameter), which is formulated as

$$D_{wake} = D(1 + 2ks) \tag{1}$$

In addition to k and s, the velocity deficit is also determined by thrust coefficient C_T, which is formulated as

$$\frac{\Delta U}{U_0} = \frac{1-\sqrt{1-C_T}}{(1+2ks)^2} \tag{2}$$

To define the value of wake decay constant, semi-empirical equation proposed by Frandsen (1992) should be used, where k equals to

$$k \approx \frac{0.5}{In\left(\frac{h}{z_0}\right)} = 0.0354 \quad (3)$$

z_0 is the roughness length of offshore areas that equals to 0.0002 according to "Terrain Roughness Classification Source" (Kollwitz, 2016). The k value calculated is 0.0354, which is quite similar to the published k value 0.040 for offshore areas in "Roughness Classification and Corresponding WDC Source" (Kollwitz, 2016).

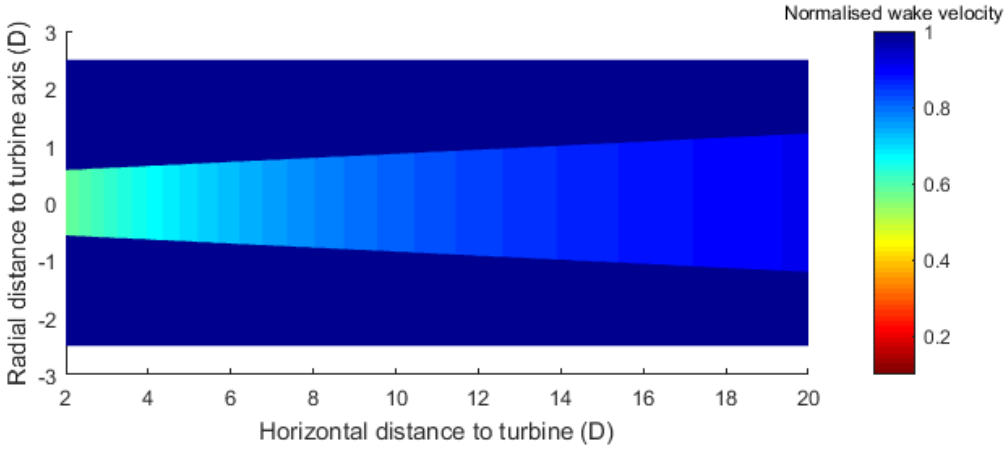

Fig. 2 Longitudinal velocity profile of Jensen wake model (U_0=10m/s, k=0.354)

As figure 2 shows, in single wake under Jensen model, the wake expansion is a linear function of horizontal distance to turbine, and the velocity deficit only relates to horizontal distance rather than radial distance to turbine axis.

2.3 Larsen Model

The Larsen model, published in 2008, is relatively new compared to Jensen model. Equations of Larsen model are derived based on the Prandtl turbulent boundary layer equations. It assumes that the wake flow is stationary, incompressible and axisymmetric, consists of three modular models: a wake deficit model, a wake meandering model and a turbine added turbulence model. The diameter of wake in the Larsen Model can be calculated by

$$D_{wake} = 2\left(\frac{35}{2\pi}\right)^{\frac{1}{5}} (3c_1^2)^{\frac{1}{5}} [C_T A(x + x_0)]^{\frac{1}{3}} \quad (4)$$

where, c_1 is a constant denoting the non-dimensional length that can be calculated by

$$c_1 = \left(\frac{D_{eff}}{2}\right)^{\frac{5}{2}} \left(\frac{105}{2\pi}\right)^{-\frac{1}{2}} (C_T A x_0)^{-\frac{5}{6}} \quad (5)$$

here, x_0 is a constant representing the turbine's position in the coordinate system that can be calculated by

$$x_0 = \frac{9.5D}{(\frac{2R_{9.5}}{D_{eff}})^3 - 1} \tag{6}$$

In the equations (6) and (7), D_{eff} is the effective rotor diameter formulated by

$$D_{eff} = D\sqrt{\frac{1+\sqrt{1-C_T}}{2\sqrt{1-C_T}}} \tag{7}$$

In the equation (6) , "$R_{9.5}$ represents the wake radius at a distance of 9.5 rotor diameters (9.5D) downstream form the turbine" (Tong et al., 2012). If the wake radius is longer than the hub height, the ground will have blockage effect on the wake expansion and the wake velocity recovery rate. $R_{9.5}$ is formulated as

$$R_{9.5} = 0.5[R_{nb} + \min(H, R_{nb})] \tag{8}$$

$$R_{nb} = \max\big(1.08D, 1.08D + 21.7D(I_a - 0.05)\big) \tag{9}$$

The deficit velocity (absolute value) can be calculated by

$$\frac{\Delta U}{U_0} = \frac{1}{9}[C_T A(x+x_0)^{-2}]^{\frac{1}{3}}\{r^{\frac{3}{2}}[3c_1^2 C_T A(x+x_0)]^{-\frac{1}{2}} - \left(\frac{35}{2\pi}\right)^{\frac{3}{10}}(3c_1^2)^{-\frac{1}{5}}\}^2 \tag{10}$$

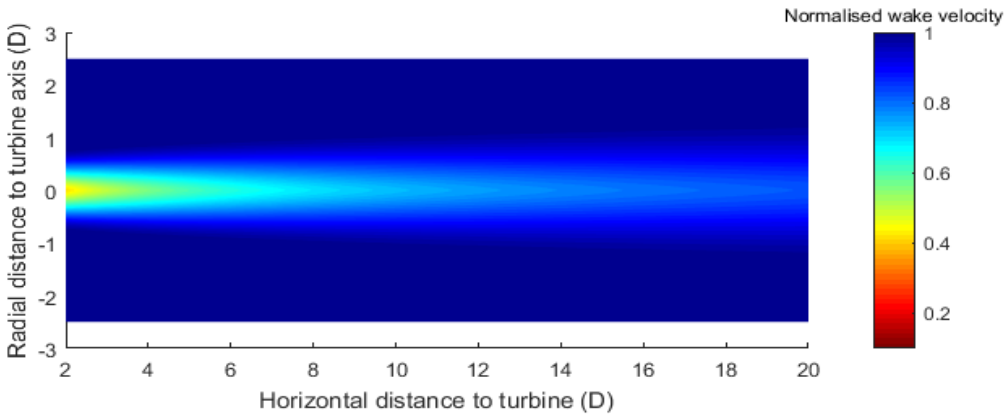

Fig. 3 Longitudinal velocity profile of Larsen wake model (U_0=10m/s, I_a=0.1)

As figure 3 shows, in single wake under Larsen model, the wake expansion trajectory is not linear, and the velocity deficit relates to both horizontal distance and radial distance to turbine axis.

2.4 Frandsen Model

Frandsen model was firstly introduced at the European Wind Energy Conference and Exhibition 2006 (Frandsen, Barthelmie, Pryor, Rathmann, & Larsen, 2006), which was designed to handle

wake field under specific conditions: wind farms of rectangular array geometry; space between units in each row and space between rows are equal; the onset wind direction is parallel to the turbine axis (horizontal turbines); rows of wind turbines are straight and parallel with each other. This model has been usually applied to large-scale offshore wind farm because of its strict application condition.

Equations of single wake in this model neglect the flow acceleration, pressure force, turbulent shear and gravity, and assumes a constant velocity profile for the section of same wake diameter. The diameter of wake can be formulated by

$$D_{wake} = D(\beta^{\frac{k}{2}} + \alpha s)^{1/k} \tag{11}$$

Where the constant k equals to 2 (square root shape) or 3 (Schlichting solution).

The wake expansion parameter β is formulated by

$$\beta = \frac{1+\sqrt{1-C_T}}{2\sqrt{1-C_T}} = (\frac{D_{eff}}{D})^2, \tag{12}$$

α can be estimated by equation

$$\alpha = \beta^{k/2}[(1+2\alpha_{(noj)}s)^k - 1]s^{-1} \tag{13}$$

where $\alpha_{(noj)} \approx 0.05$ (Frandsen et al., 2006)

The velocity deficit is formulated as

$$\frac{\Delta U}{U_0} = \frac{1}{2}\left(1 \pm \sqrt{1-2\frac{A}{A_{wake}}C_T}\right) \tag{14}$$

For the simulation follows, only situation that induction factor a>0.5 has been considered, so in equation (14), only "+" is be used.

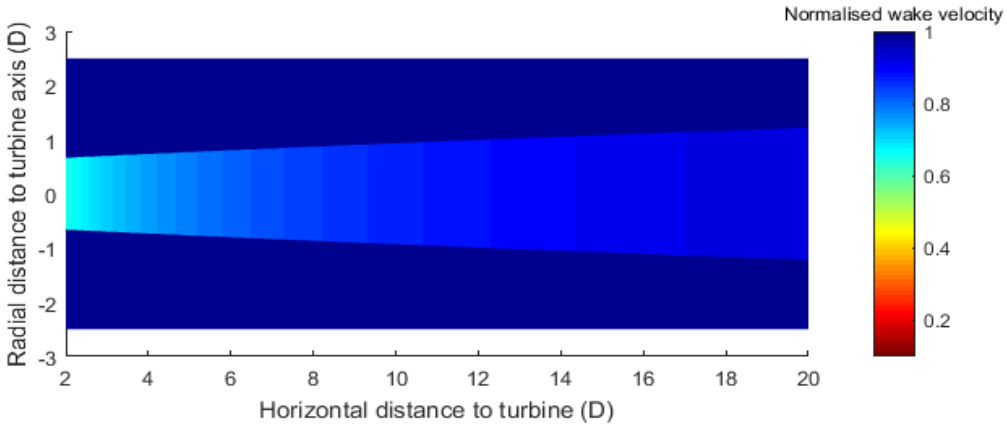

Fig. 4 Longitudinal velocity profile of Frandsen wake model (k=2, α=0.7)

As Figure (4) shows, depiction of wake field of Frandsen wake model is quite similar to Jensen model, that also ignores the relationship between velocity deficit with radial distance, and the wake expansion trajectory is also linear.

2.5 Ishihara Model

The Ishihara model was proposed based on a wind tunnel test with 1/100 scale turbine model, and considers three major parameters: thrust coefficient C_T, ambient turbulence I_a and mechanical generated turbulence I_w. It indicates that a higher C_T induces a higher velocity deficit but higher I_a and I_w increases the rate of wake recovery. (Ishihara, Yamaguchi, & Fujino, 2004)

The diameter of wake is formulated as

$$D_{wake} = \frac{k_1 C_T^{\frac{1}{4}}}{0.833} D^{1-\frac{p}{2}} x^{\frac{p}{2}} \tag{15}$$

$$\mathrm{p} = k_2(I_a + I_w) \tag{16}$$

$$I_w = \frac{k_3 C_T}{\max(I_a, 0.03)} \left\{1 - \exp\left[-4\left(\frac{x}{10D}\right)^2\right]\right\} \tag{17}$$

Where the constants k_1, k_2, and k_3 equals to 0.27, 6.0 and 0.004, and I_a equals to 0.06 for offshore wind farm respectively. (Ishihara et al., 2004)

The velocity deficit is formulated as

$$\frac{\Delta \mathrm{U}}{U_0} = \frac{\sqrt{C_T}}{32}\left(\frac{1.666}{k_1}\right)^2 \left(\frac{x}{D}\right)^{-p} \exp\left(-\frac{r^2}{{D_{wake}}^2}\right) \tag{18}$$

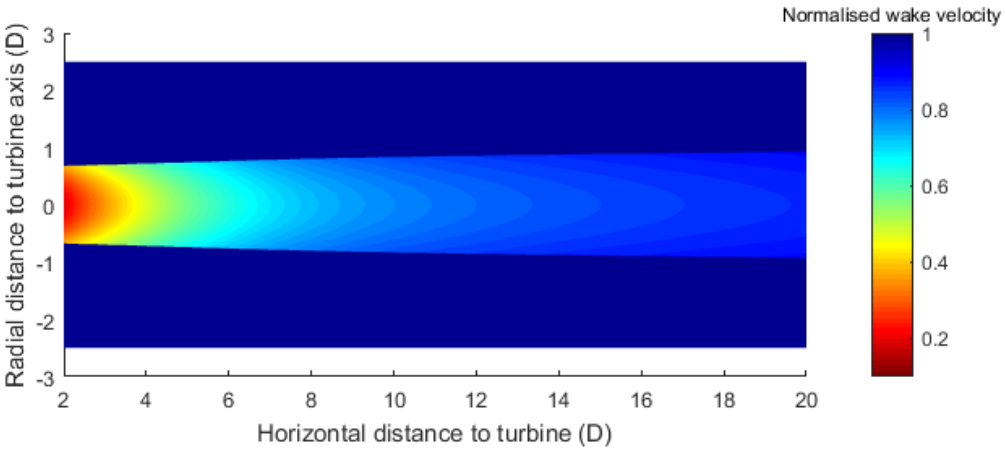

Fig. 5 Longitudinal velocity profile of Ishihara wake model

Ishihara wake model cannot be used when horizonal distance is shorter than 2D, otherwise the velocity calculated will be negative, which is obviously unreasonable.

As these four longitudinal profiles show, when the horizontal distance to turbine is long enough that exceeds 10D, the velocity value estimated by four models is almost same. The position nearer to turbine within wake, the difference between four velocity fields is more obvious. In order of average speed from low to high when horizontal distance is within 10D, the sequence of wake models is Ishihara, Larsen, Jensen and Frandsen.

2.6 Wake Superposition methods:

As figure 6 shows, when two or more than two turbines are inline or partly-offset, different wakes generated by different turbines will overlap with each other, that is why wake merging models are needed to show the interacting effect between different turbines within an array.

As shown below, there are three most commonly used single wake superposition methods in commercial analytical software given in form of equations (19), (20) and (21) (Gunn et al., 2016)

$$\text{Largest deficit: } U_{norm} = \min\left(u_{norm,1}, u_{norm,2}, \dots\right) \tag{19}$$

$$\text{Root} - \text{sum} - \text{square: } U_{norm} = 1 - \sqrt{\sum \left(1 - u_{norm,i}\right)^2} \tag{20}$$

$$\text{Linear: } \mathrm{U}_{norm} = 1 - \sum \left(1 - u_{norm,i}\right) \tag{21}$$

These three methods consider little from the aspects of the flow physics, but the flow velocity fields established based on these three models are still quite accurate compared to CFD simulation result. Three combination methods will be tested in Larsen model because of its relative higher accuracy in depicting velocity field according to radial distance.

There are other new and innovative wake models that not be introduced in this thesis like 3-D wake model published in (Sun & Yang, 2018a).

The equations and parameters in the four classical wake models and the three wake superposition methods are well established in existing literature that can be used directly. Similar works to test different analytical wake models in power loss calculation have been made in (Archer et al., 2018), but without consideration of different operation strategies.

3 Development of a Wake Model

Four different analytical wake models: Jensen, Larsen, Frandsen and Ishihara models will be established and three different wake combination methods: Largest Deficit, Root-Sum-Square,

Linear will be tested in this thesis, whose equations are well developed and verified in relative literature. The thesis will compare the four models with detailed CFD simulation results to decide which one is more accurate in wake field assessment. Similar research has been completed by (Tong et al., 2012), but without systematic comparation with CFD model and further application to a specific wind turbine array to calculate energy yield under different operation strategy.

CFD simulation result published in existing literature (Gunn et al., 2016) is a good benchmark to use. Four simple but representative different cases: Single wake, two turbines inline, two turbines partly offset and two turbines fully offset have been studies, as figure (6) shows (x=8D, y=1D, y'=1.75D). An overall summary of comparison of velocity field under different conditions has been represented clearly in form of chromatic cross section in the following text.

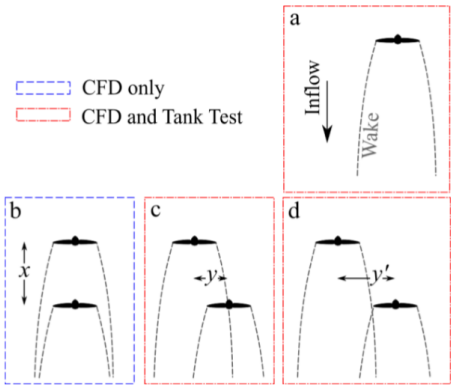

Fig. 6 Schematic diagram of CFD simulation (Gunn et al., 2016)

To decide which wake model is more accurate in characterizing the wake field and which single wake combination method is more reliable to reflect the mutual effect between different single wake, these four models should adopt the same parameters (as table 2 shows) of CFD simulation. Then, different wake combination method will be used to simulate the interacting effect between different wakes and the simulated velocity field will be compared with CFD simulation result in chapter 2 and chapter 3.

Table 2 Summary of CFD parameters that used in analytical wake models

Bulk flow wind speed	12.0 m/s	Turbulence intensity	5.26%
Rotor diameter	126 m	Rotor hub height	90 m

3.1 Single Wake Model Implementation and Evaluation

For one specific wind turbine (D=126m, h=90m), under stable onset wind along with horizontal axis (U_0=12m/s), the wake expansion rate and velocity recovery rate are different based on

different wake models. Three representative C_T values 0.80, 0.45 and 0.15 are chosen to test the sensitivity level of the four wake models mentioned above.

As figure 7, 8, 9 show, wake expansion rate is not sensitive to the variation of C_T, especially for Jensen, Larsen and Frandsen wake models. For Ishihara wake model, the influence of C_T on wake diameter's increase behind wind turbine is relatively obvious, but still not significant enough. However, velocity deficit and wake velocity recovery rate are very sensitive to the variation of C_T, especially for Larsen wake model. Both the velocity deficit and the wake velocity recovery rate increase as C_T increases. Higher C_T means that a wind turbine extracts more energy from the air flow, which induces a more significant decrease in velocity as wind flows through the turbine, but also generates higher mechanical turbulence that accelerate the wake velocity recovery process.

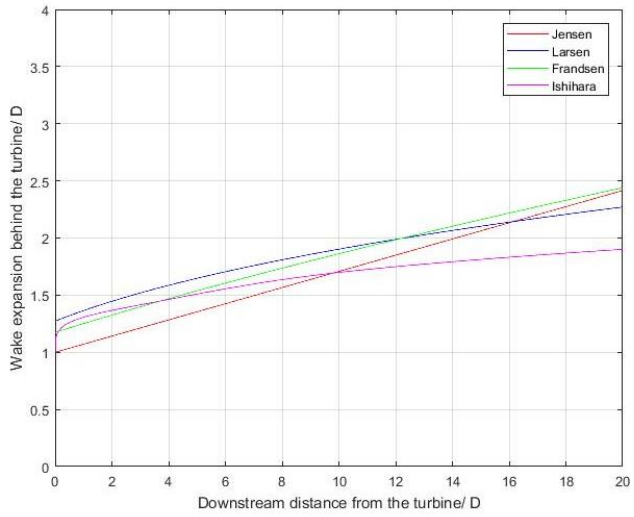

Fig. 7-a Wake expansion profile- C_T=0.80

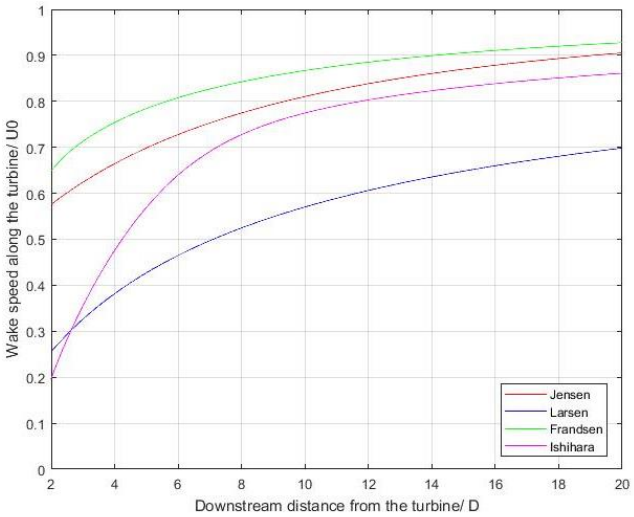

7-b Wake velocity profile- C_T=0.80

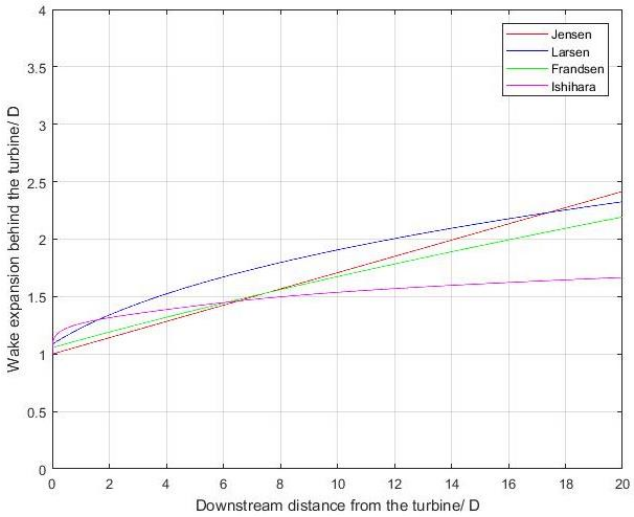

Fig. 8-a Wake expansion profile- C_T=0.45

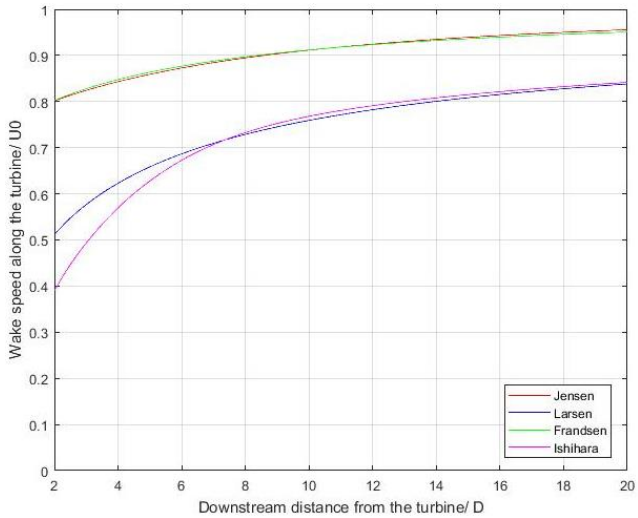

8-b Wake velocity profile- C_T=0.45

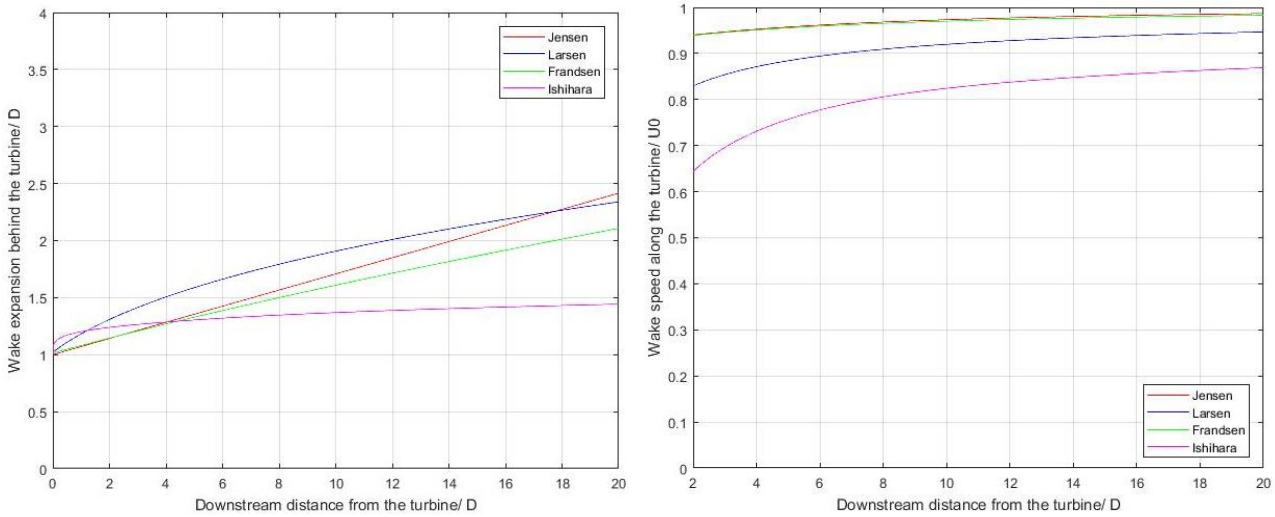

Fig. 9-a Wake expansion profile- C_T=0.15 9-b Wake velocity profile- C_T=0.15

As figure 10 shows, for a single wake, under same condition, the velocity fields presented by transverse profile are quite different according to different wake models. The size of turbine is exactly the same in each transverse profile that is shown as a black circle in the center of single wake. The blockage effect of ground is very complex that can alter the shape and speed of wake, although has been considered in the CFD simulation, has not been considered in these four analytical wake models. As a result, only the upper part of wake that higher than turbine axis should be compared to decide which model is closer to CFD simulation method.

First of all, Larsen model is better to reflect the relationship between radial distance with velocity deficit. In real situation, velocity deficit would decrease as radial distance increases, which means the velocity in the center of wake is always the lowest. This relationship also can be seen in Ishihara model but in much vaguer way. To the opposite, in Jensen model and Frandsen model the velocity is same for one cross section. Because of this attribute, Larsen model is the best choice to test wake superposition methods.

Secondly, from the transverse profiles, Frandsen model is the most reasonable one from the perspective of wake expansion rate. The wake diameter looks much smaller in Larsen model than in CFD simulation and the other 3 models, but actually, the diameter of wake is very close in the four models when the C_T is high as 0.914. Because in the outer part of wake in Larsen model, the wind normalized velocity is too close to 1, so the wake edge is not obvious enough in the transverse profile.

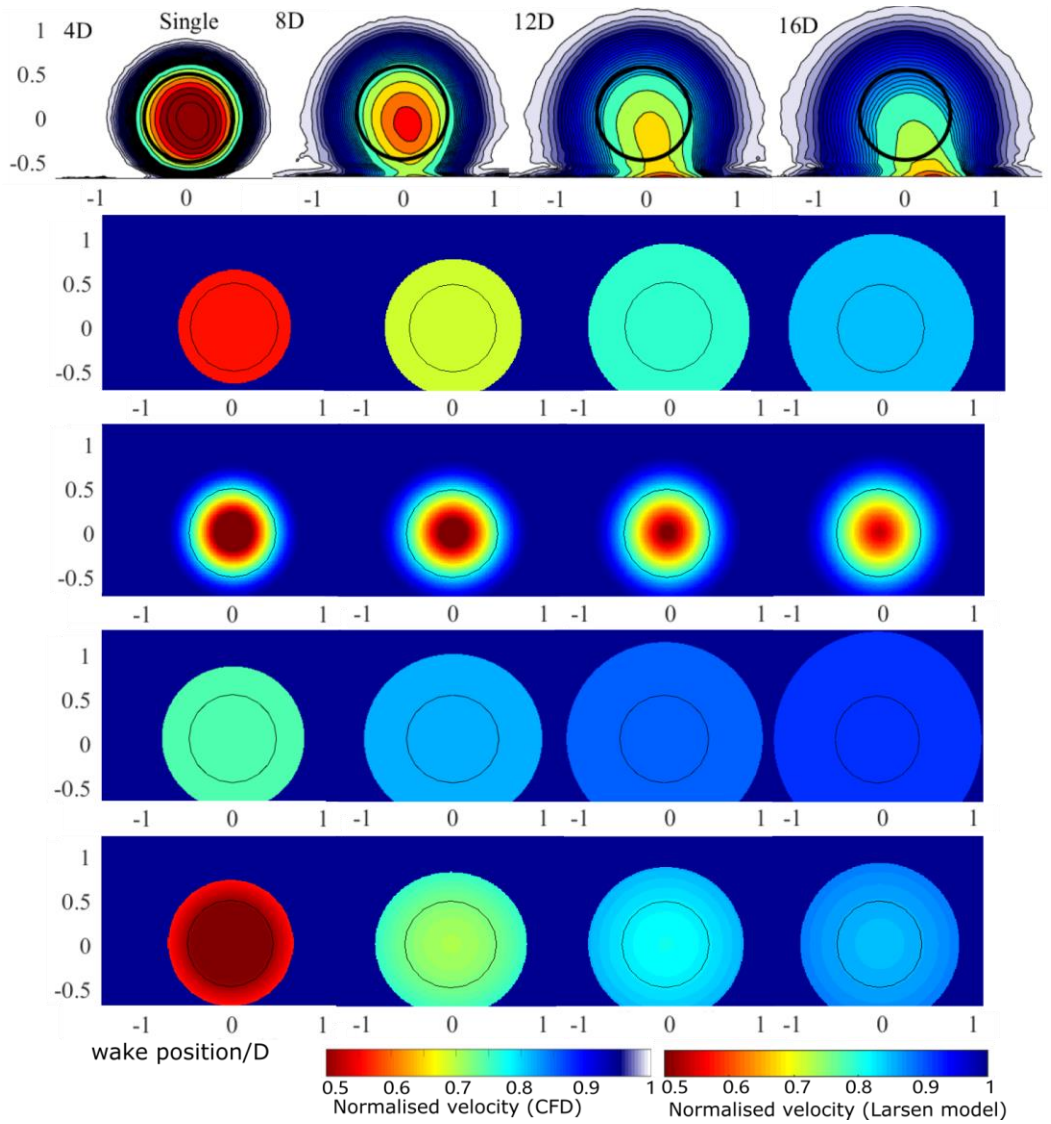

Fig. 10 Comparison between velocity fields based on different wake models (from top to bottom, are transverse profiles of CFD simulation (Tong et al., 2012), Jensen wake model, Larsen wake model, Frandsen wake model and Ishihara wake model simulation result when C_T=0.914)

At last, the average velocity in Jensen, Larsen and Ishihara is more accurate than Frandsen model. To test the single wake's influence on the downstream turbine, four models have been used under the two turbine partly offset condition (horizontal distance=8D). The least sensitive wake model according to the relationship between equivalent onset velocity of downstream turbine as the two turbines' center distance increases is Frandsen model. As figure 11 shows, the other three models are quite sensitive for this relationship (at a similar sensitivity level). In the other three models, the equivalent onset velocity of downstream turbine is highest in Larsen model, is moderate when use Jensen model and is lowest when use Ishihara model.

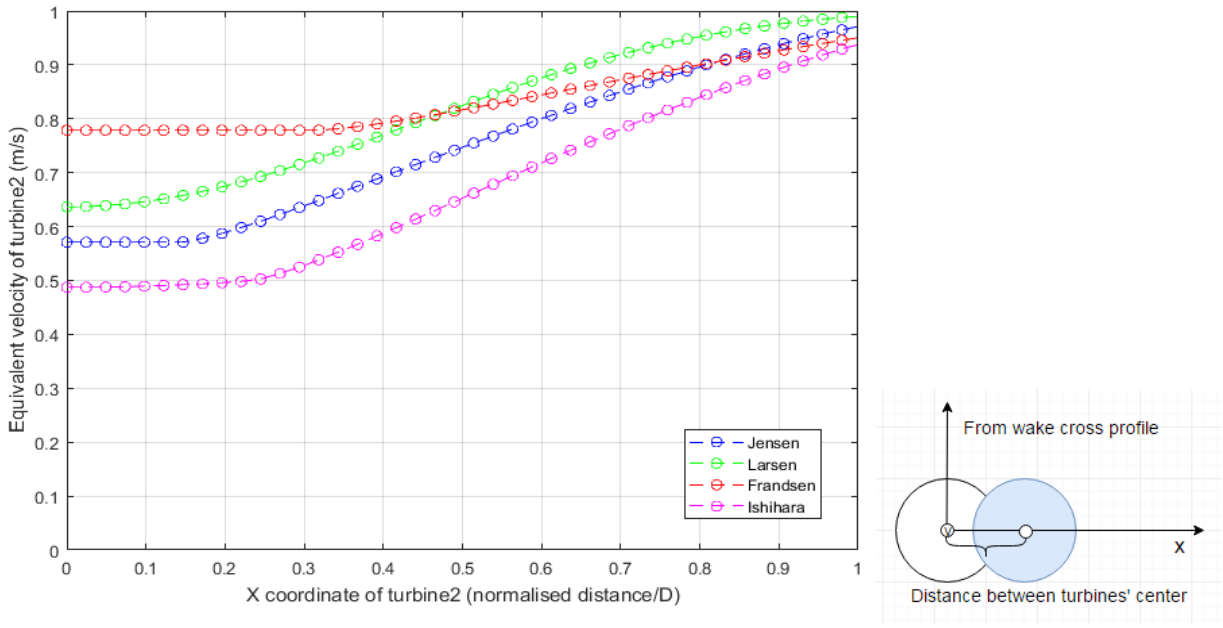

Fig. 11 The equivalent velocity of downstream turbine when it is partly offset

In conclusion, the Larsen model is best according to single wake analysis.

3.2 Multi-wake Model Implementation and Evaluation

Based on the results of applying the four models to the single wake field and the comparison with the CFD simulation results, it is concluded that Larsen model is the most accurate analytical model to simulate wake field, as in which, the values of all parameters are consistent with the CFD simulation, presented in Chapter 2. However, more complex situation should be considered to decide which wake combination method is the best. Three common but widely-used methods referred to as Largest Deficit, Linear and Root-Sum-Square will be tested for multiple wake based on Larsen model and be compared with CFD simulation result in the following text. In all the three situations, the C_T is 0.904 for the upstream turbine, and C_T is 0.859, 0.968 and 0.917 for the second turbine in inline, partly offset and fully offset situation respectively. The results are shown below, and the coordinates, scales and colors in these figures are designed consistently to make comparison easier.

As figure 12 shows, for two-turbine situation, the CFD can simulate the wake field when the wake position is exactly at the position of downstream turbine, 8D. The velocity deficit is largest at the edge of the downstream turbine, where the lift and thrust force is highest for the airfoils, just the opposite of the fully formed wake. Unfortunately, Larsen model, or any other types of analytical

model cannot simulate wake within the same plane of turbine itself. As a result, only situations of 12D and 16D will be considered to test 3 superposition methods based on Larsen model.

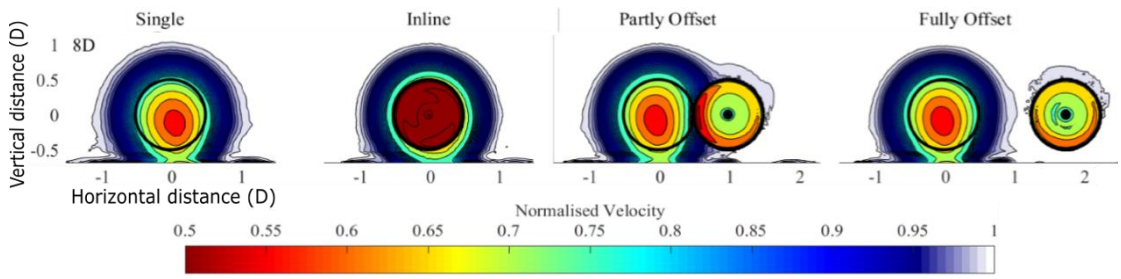

Fig. 12 CFD Simulation result when 2 turbines distance is 8D (Gunn et al., 2016)

As mentioned before, because the wake edge cannot be presented properly in the cross-section figure in Larsen model, especially when the horizontal distance between two turbines is large as 1.75D as employed in the CFD simulation, interaction between two wakes cannot be distinguished by the naked eye, as figure 13 shows. Therefore, for the fully offset situation, y'=1.4D is chosen for turbines position in the following simulation, and all the other parameters are the same with CFD simulation.

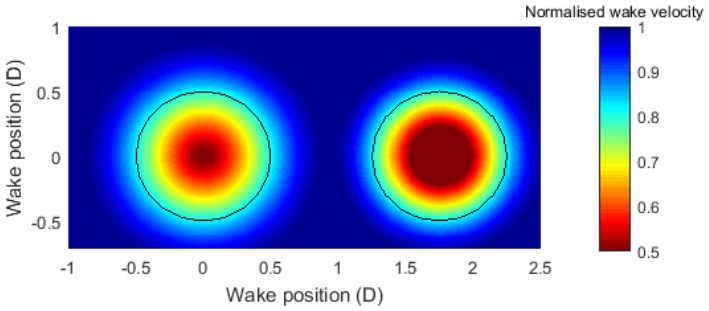

Fig. 13 Transverse profile of wake field when two turbines are partly offset_8D

No matter what kind of wake combination method is used, the wake region remains the same, in other words, wake combination method only affects the overlapping area of different wakes. As figure 14 shows, according to velocity deficit from low to high, the sequence of methods is: Linear, Root-Sum-Square (RSS) and Largest Deficit. In linear superposition method, the interaction between different wakes is the strongest, whose color in transverse section is closest to the CFD simulation results.

Based on the single wake test (section 3.1) and multiple wake test (section 3.2), analytical wake model Larsen model and Linear superposition method are chosen for the further test to find best operation strategies for 4-turbines array unit.

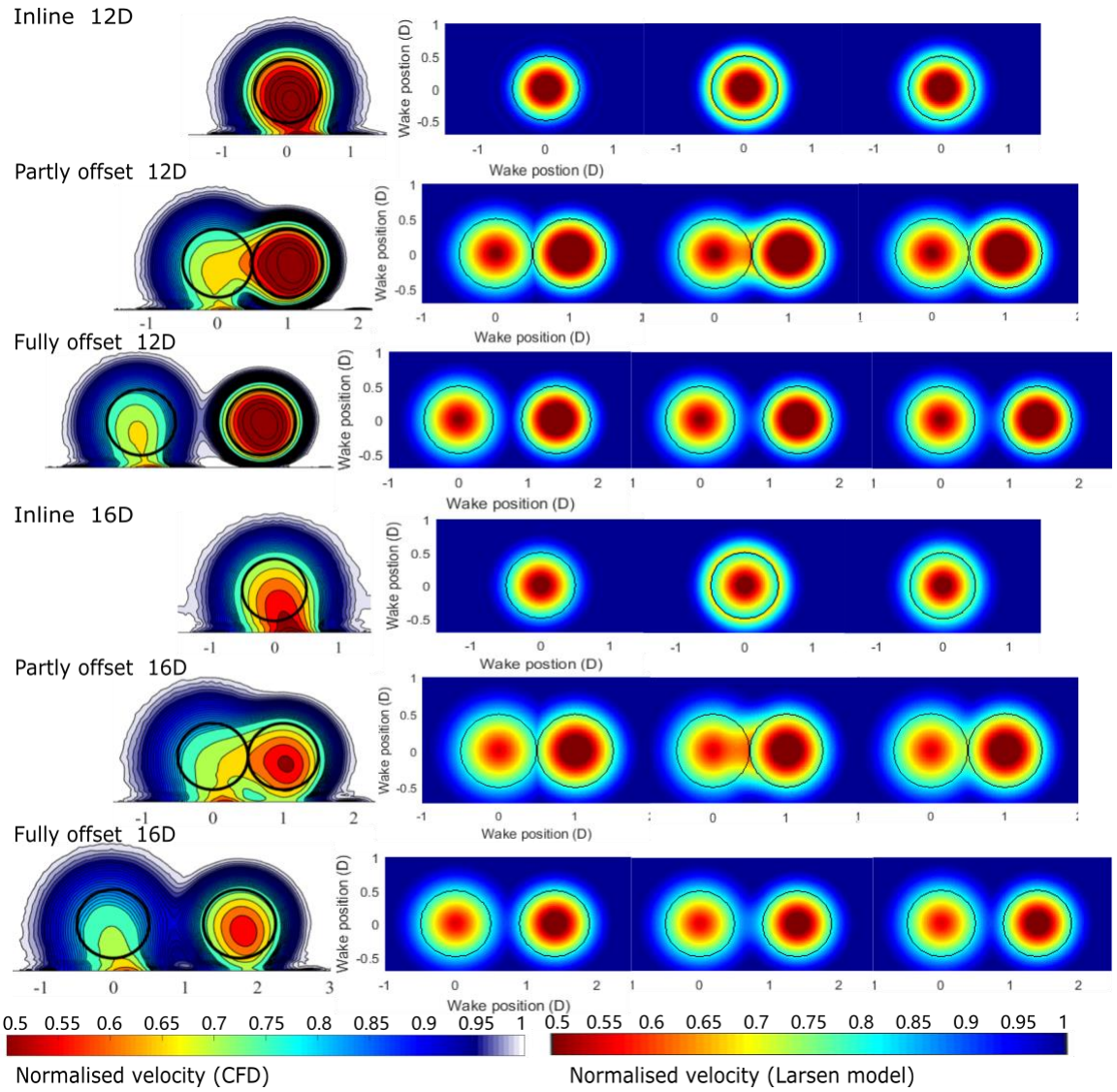

Fig. 14 Comparison between velocity fields based on different wake combination methods (the left hand frame is from Gunn et al and the right hand frames are from the implementation of the models in Tong et al. 2012: Largest Deficit, Linear, Root-Sum-Square combination methods)

4 Effect of Operation Strategies on Power Generation

4.1 Reference Wind turbine

In CFD simulation mentioned above, the value of C_T is high and fixed, which is not practical for real operation of wind turbine. On the other hand, the strong correlation between wind speed and thrust coefficient cannot be ignored. For power output analysis, parameters of real wind turbine Vestas V80-2MW should be adopted in terms of availability of data to give more reliable

estimation of power output. The hub height of reference turbine is 80m and the rotor diameter is 80m; with pitch and yaw regulation, it can work under wind of variable speed from variable direction (Vestas, 2011).

By fitting the curve in figure 15, we can get the relationship between wind speed (U/ m/s) and C_T for the turbine for the optimal performance situation, which can be compared with simulation results later, as equation (22) shows:

$$when\ 4 \le U < 10\ \mathrm{m/s}, C_T = 0.8;$$

$$when\ 10 \le U < 12.2\ \mathrm{m/s}, \quad C_T = -0.0538 \cdot U + 1.3164;$$

$$when\ 12.2 \le U < 12.5\ \mathrm{m/s}, C_T = -0.0844 \cdot U^2 + 1.7201 \cdot U - 7.7845;$$

$$when 12.5 \le U < 25\ \mathrm{m/s}, \quad C_T = 3.4868 \cdot e^{-0.172U}; \qquad (22)$$

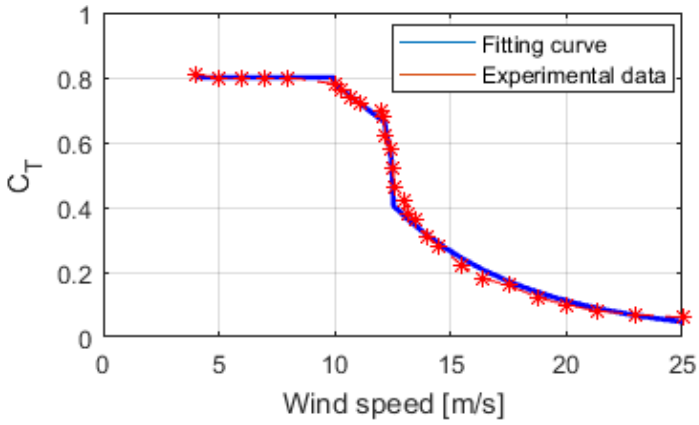

Fig. 15 Thrust coefficient CT for Vestas V80-2MW wind turbine- based on (N. Moskalenko, Rudion, & Orths, 2010b)

The rated power of the turbine is 2MW, cut-in wind speed is 4m/s, rated wind speed is 16m/s and cut-out wind speed is 25m/s. By fitting the published power curve, the power (P/ kW) of the turbine can be calculated by wind speed (U/ m/s) based on equation (23) for the optimal power output, and this equation can only be applied to the last downstream turbine in power output simulation.

$$P = -3.4939 \cdot U^3 + 96.804 \cdot U^2 - 608.43 \cdot U + 1132.1\ , when\ \ 4 \le U \le 15\ \mathrm{m/s};$$

$$P = 2000, when\ 15 \le U \le 25\ \mathrm{m/s}; \qquad (23)$$

C_T and C_P have strong correlation according to the "Linear Momentum Theory", as following equations show:

$$C_T = 4\alpha(1-\alpha)^2; \qquad (24) \qquad C_P = 4\alpha(1-\alpha); \qquad (25)$$

The derivation of the equations (24) and (25) is based on the Bernoulli equation and conservation of mass, conservation of momentum, conservation of angular momentum, and conservation of energy. As such, this equation does not fully describe the relationship between thrust and wake velocity across the full range of turbine operating points. Since losses due to drag and wake rotation are neglected this approach is most accurate for high values of power coefficient, typically at wind speeds less than rated speed. For a specific turbine geometry, pitch regulation is generally applied at wind speeds greater than rated speed. For these operating points the relationship between C_P, C_T and wake velocity is more complex than in the optimal performance situation and so the direct application of linear momentum theory is limited.

For this range C_p and C_T can instead be related by Blade Element momentum theory. However, this requires information on the turbine geometry in the form of the radial variation of blade geometry, chord length and twist angle. This information is not available for all commercial turbines for which the published information is typically the power curve. Instead a generic 2 MW turbine available as an exemplar model in the design software DNV GL Bladed is employed as a reference case. The principle dimensions are comparable to those of a 2 MW which also has the hub height of 80m, rotor diameter of 80m and rated power of 2MW will be tested under different pitch angle to generate CT and CP curves in the case of not the optimal performance according to wind speed. Therefore, the power of upstream turbines can be calculated by different C_P curve under different pitch angle.

By changing the pitch angle from -5° to 10° and performing the C_T simulation under different TSR, C_T curves of the Bladed Demo_A 2MW reference turbine have been made, as figure 16 shows.

In practice, the independent variable defining turbine performance is the onset wind speed and TSR should be selected for a given wind speed. This is done by the following approach. It is assumed that the rotational speed of the wind turbine is fixed. This simplification is not strictly the case but generally applies over the range of wind speeds of interest ($U > U_{rated}$) and has limited effect on the predicted parameters for other values of wind speed (Takahashi et al., 2010).

Tip Speed Ratio is defined as $\mathrm{TRS} = \omega \mathrm{R}/\mathrm{U}_0$, $\omega_{rotor} = 2\pi n = 2 \times 3.14 \times 1500 \div 60 = 157 rad/s$, $\text{ratio} = \frac{\omega_{generator}}{\omega_{blade}} = 83.33$, $\therefore \ \omega_{rotor} = 1.88 \mathrm{rad/s}$, $\therefore TSR = \frac{\omega R}{U_0} = \frac{75.2}{U_0}$, $\therefore U_0 =$

$\frac{75.2}{TSR}$. By the same method, C_T and C_P curves according to different wind speed and pitch angle can be shown in figure 17 and 18.

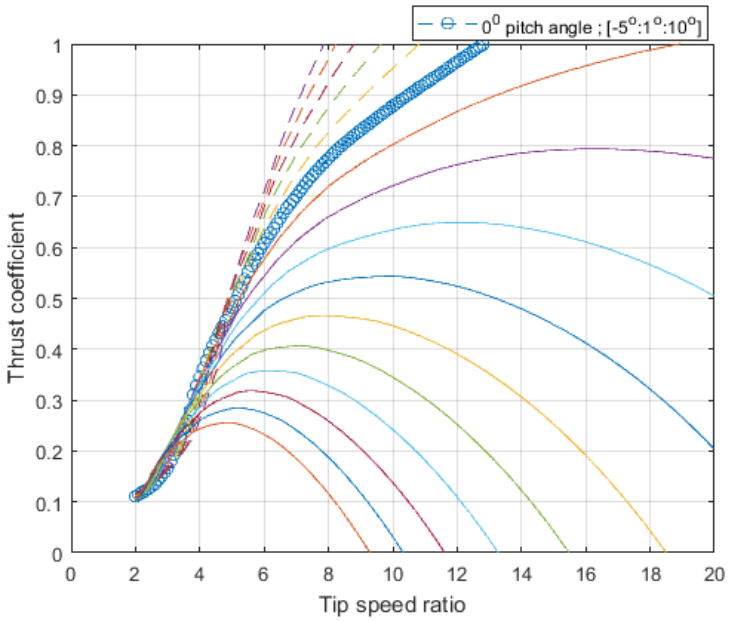

Fig. 16 C_T curves of the Bladed demo_a 2MW reference turbine (dashed line=negative pitch angle; solid line=positive pitch angle; above 0° pitch angle line, the pitch angle gradually decreases to -5° (purple dashed line); below 0° pitch angle line, the pitch angle gradually increases to 10° (red solid line); gradient is 1°), the same in Fig. 17

As figure 17 shows, for the reference turbine, the range of C_T is much higher when wind speed is below the rated wind speed. In other words, the pitch regulation has very limited ability to regulate C_T and velocity deficit when wind speed is greater than 15m/s. When the wind speed is lower than 16m/s, the larger the pitch angle, the smaller the C_T.

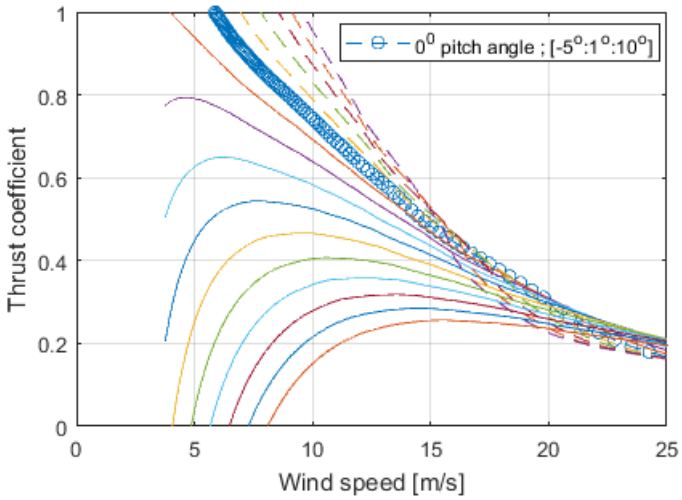

Fig. 17 C_T curves of the Bladed demo_a 2MW reference turbine

As figure 18 shows, the effect of pitch angle on C_P is very different, no matter what is the wind speed, pitch angle has always been very strong in regulating C_P. Basically, the case of 0° pitch angle is almost consistent with the case of optimal performance C_P curve when the wind speed is lower than 18m/s, which means any operation that alter pitch angle from zero degree will decrease the power output of the turbine. However, only positive pitch angle will be meaningful when wind speed is less than about 16m/s, because only positive pitch angle can decrease the C_T of upstream turbine and produce less velocity deficit. The same situation when wind speed is high than 16m/s, because by increasing the pitch angle from zero degree can increase the C_P as much as possible while reducing the C_T.

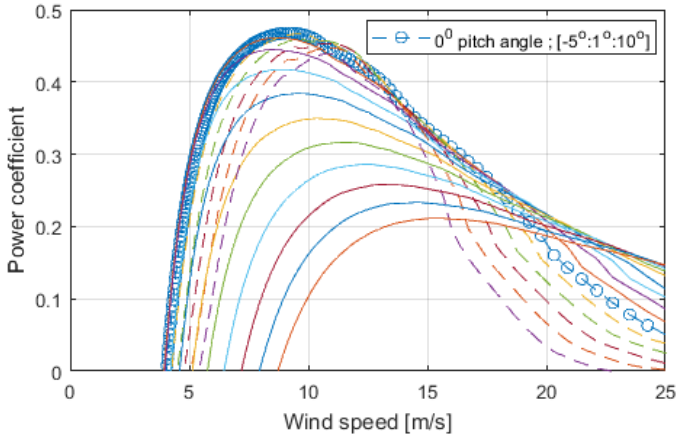

Fig. 18 C_P curves of the Bladed demo_a 2MW reference turbine

(dashed line=negative pitch angle; solid line=positive pitch angle; for wind speed from 5 to 10 m/s, below 0° pitch angle line, the pitch angle gradually decreases to -5° (purple dashed line); below 0° pitch angle line, the pitch angle gradually increases to 10° (red solid line); gradient is 1°)

Analysis in the next section of the effect of turbine operating point on downstream wake and hence power output and loading of an array is based on the C_T and C_P curves in figure 17 and 18, rather than on Linear Momentum Theory.

4.2 The Effect of Pitch Regulation on Wake and Power Output of Two Turbines

Two typical configurations of two turbines, inline and partly offset, are considered, and for each situation the individual and total power output of the two types of array are calculated for a range of pitch angles based on Larsen model, existing C_T and C_P curves of the reference turbine. Predicted performance of each turbine will then be shown in the form of charts in order to observe the relationship between total power output and operation strategies.

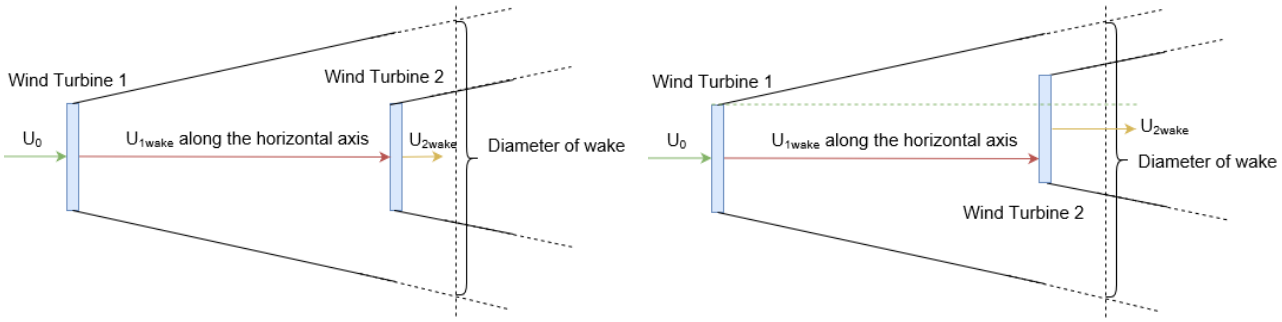

Fig. 19 Schematic diagram of the two test cases (in line& partly offset)

As figure 19 shows, the two turbines are in-line according to the onset wind direction and the distance between them is 8D in the first case.

Conceptually, higher C_P of the second turbine and lower C_T of the first turbine will benefit the power output of the second turbine. Higher C_T will induce stronger deficit velocity behind this specific turbine. As a result, for the first turbine, higher C_T is always preferred due to the corresponding increase of Cp, but for the downstream turbine, lower C_T of the first turbine is preferred as this allows a greater onset velocity and hence power output to the downstream turbine.

For the best solution in order to get the maximum power output, C_T for the first turbine cannot be either too high or too low. It should balance the performance of both turbines. As a result, in order to attain maximum power output of two turbines, the C_P should be set at the maximum value for downstream turbine, and C_T and C_P for upstream turbine should be alterable, which are the key factors to decide the maximum total power output. In order to verify the above conjecture, three sets of simulation will be implemented next.

Three representative situations, wind speed is 7.5m/s (much lower than rated speed (or just 50% of U_{rated})), 15m/s (rated speed) and 21.5m/s (much higher than rated speed (or just approx. 150% of U_{rated})) respectively, will be considered. For example, when wind speed is 7.5 m/s, corresponding 16 different C_T and C_P under pitch angle from -5° to 10° can be found in figure 17 and 18, then each pair of C_T and C_P under a particular pitch angle will be tested in simulation based on Larsen model.

On one hand, the generator type of the reference turbine is 4-pole doubly fed generator (slip rings), which can improve the system efficiency by up to 10% (Müller, Deicke, & W., & Rik Doncker,

2002). The efficiency of double fed generator is very high, and if it is assumed as 1, the power output of upstream turbine can be calculated by equation $P = \frac{1}{2}\rho A {U_0}^3 \cdot C_P$. Then, for wind speed from cut-in speed 4m/s to cut-out speed 25 m/s under pitch control from -5° to 10°, all possible power of the turbine can be calculated, as figure 20 shows. Obviously, only the part in the black rectangular box is reasonable (higher than 0MW and lower than 2MW). The optimal power output points under different wind speed can be found in figure 20 and the calculated optimal power curve is shown in figure 21.

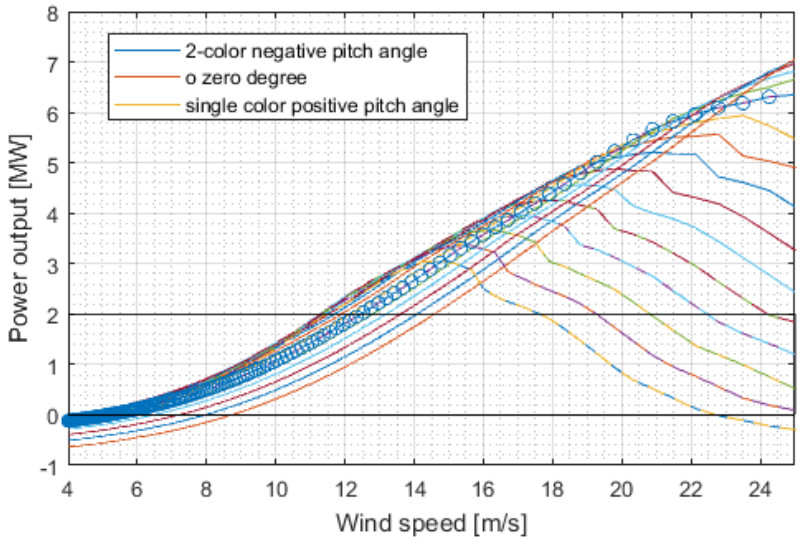

Fig. 20 Power curves under pitch regulation calculated by $\frac{1}{2}\rho A {U_0}^3 \cdot C_P$

(the lowest red solid line is of pitch angle 10°, the lowest blue-orange colorful line is of pitch angle -5°, the gradient is 1, the sequence of pitch angle changes in sequence)

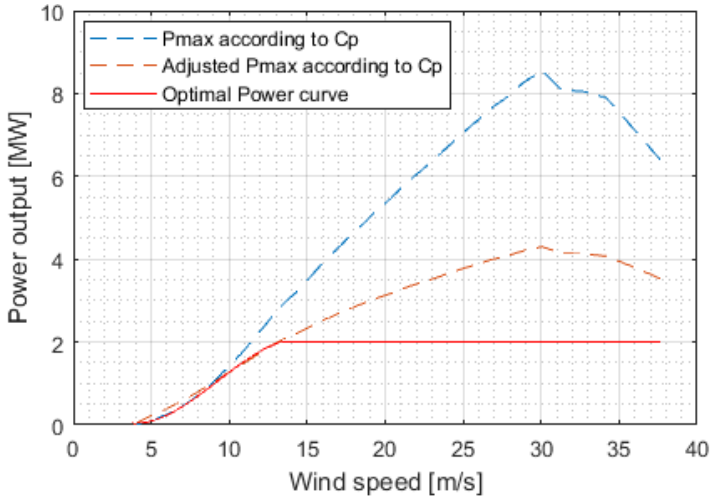

Fig. 21 Comparison between calculated, adjusted calculated and actual power curve

Reference wind turbine power curve-based on (Vestas, 2011)

As figure 21 shows, the calculated curve and actual optimal curve are in good agreement in the interval where the wind speed is lower than 9 m/s, but after 9m/s, it is much higher than the actual curve (rated power). As a result, the equation $P = \frac{1}{2}\rho A {U_0}^3 \cdot C_P$ is not reliable to use here, but need be improved to fit the actual optimal power curve. That is because $P = \frac{1}{2}\rho A {U_0}^3 \cdot C_P$ is the aerodynamically accessible power from wind, the real power output of turbine is much lower since the limits of gear box, rotor and tower, especially when onset wind speed is high.

Finally, the equation to simulate power output of upstream turbine is defined as:

$$P = \frac{1}{2}\rho A {U_0}^3 \cdot C_P, \qquad \text{when } U_0 \le 9m/s;$$
$$P = \left(\frac{1}{2}\rho A {U_0}^3 \cdot C_P\right)^{0.68}, \text{when } U_0 > 9m/s;\ if\ P \ge 2\ MW, P == 2MW; \qquad (26)$$

On the other hand, using the same method in Single Wake Test (section 3.1), equivalent onset velocity for downstream turbine can be calculated, so its power output can be estimated based on the power curve in figure 21 (optimal performance curve). Therefore, the best pitch angle that gives the maximum total power output for these two turbines will be known by comparing 16 simulation results (16 pitch angles).

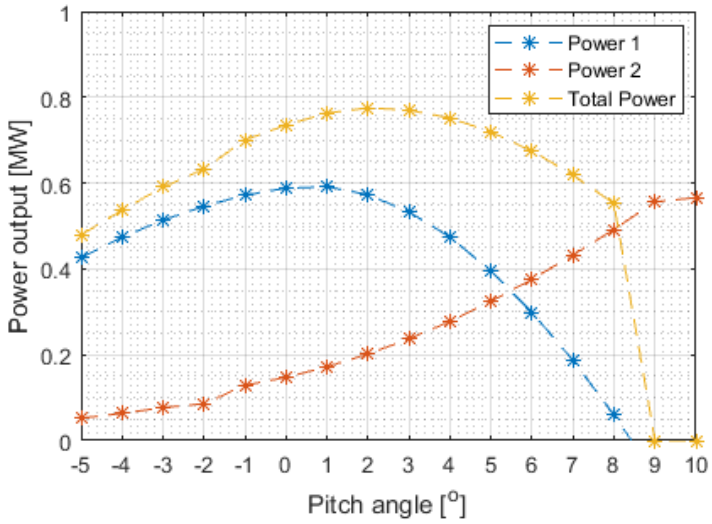

Fig. 22 Power output under pitch control from -5°to 10°_U_0=7.5m/s

When the onset velocity U_0 is 7.5m/s (TSR=10), for upstream turbine, the power output increases as pitch angle increases firstly and reaches its maximum value 0.5913 MW at 1° pitch angle, then it decreases to 0 MW as pitch angle exceeds 8° . Meanwhile, since higher pitch angle of upstream turbine induces lower C_T, the velocity deficit caused by upstream turbine decreases, and power

output of downstream turbine increases continuously. Total power output of the 2 turbines reaches its maximum value 0.7750 MW when pitch angle of first turbine is 2°, which is 11.9 kW higher than the situation of optimal performance of upstream turbine.

When onset velocity U_0 is 15 m/s (TSR=5), the maximum total power output corresponds to the optimal performance point of the upstream turbine when pitch angle equals to 7° and both turbines can operate around rated power.

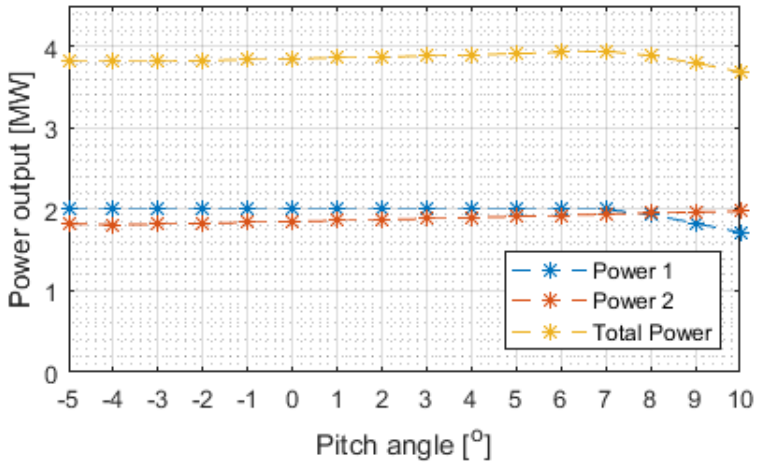

Fig. 23 Power output under pitch control from -5°to 10°_U_0=15m/s

When U_0 is 21.5 m/s (TSR=3.5), pitch angle from -1° to 10° all can satisfy the maximum power output of both turbines, because the velocity deficit can hardly affect the second turbine (always be exposed to velocity higher than rated speed) when onset wind U_0 speed is high enough.

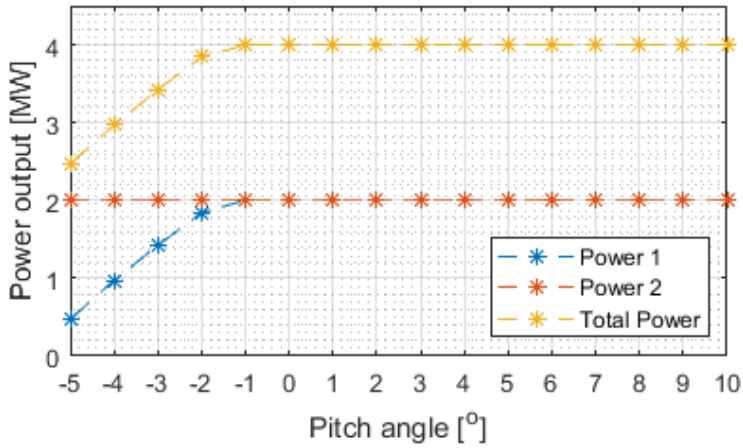

Fig. 24 Power output under pitch control from -5°to 10°_U_0=21.5m/s

As figure 25 shows, because the effect on the equivalent onset velocity for downstream turbine caused by pitch control of the upstream turbine is not very obvious (always within 4 m/s difference), only in the interval where the power changes rapidly with speed (when $U_0 \leq 13m/s$)

the pitch control is influential. In addition, when the onset velocity U_0 for upstream turbine is low, the equivalent onset velocity for downstream turbine changes more under pitch control. Under these two effects, pitch control is more meaningful for low U_0.

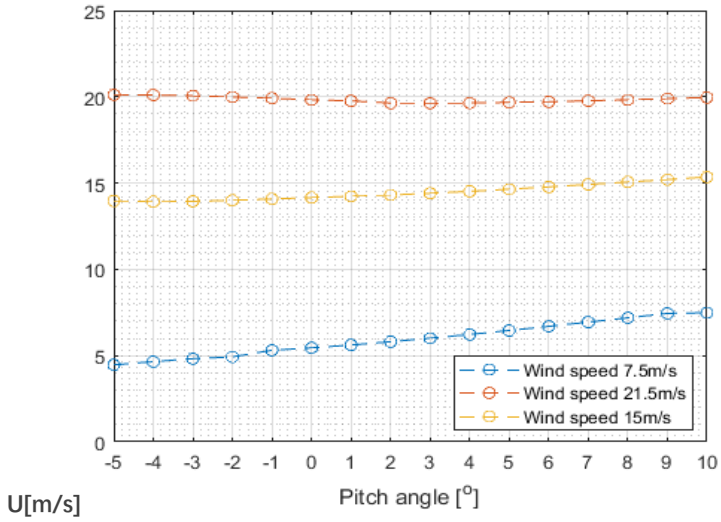

Fig. 25 The equivalent onset velocity for downstream turbine under pitch control

By testing the total power output under different U_0, best C_T for upstream turbine can be found. As figure 26 shows, a slightly decreased C_T (change within 0.2) from the level of optimal C_T for the upstream turbine always benefits the total power output for the two turbines when the onset wind speed is below rated speed (15 m/s). For wind speed higher than 15 m/s, the C_T of optimal power performance of upstream turbine can be adopted directly, almost having no effect on the total power output for the two turbines. On the whole, except for wind speeds of 5 m/s and 10 m/s, the change in pitch angle is natural that it gradually rises and then falls. Correspondingly, there are only two points of abrupt change in C_T curve for maximum total power output. However, smooth adjustment of pitch angle or C_T is more common and practical for wind turbines, rather than this kind of abrupt change. In real operation, the value of C_T at the wind speed of 5 m/s and 15 m/s will be adjusted to 1 and 0.45 respectively to avoid abrupt pitch angle's change.

Partly-offset is the more common situation than the first inline case (y'=0.5D). The method to calculate the total power output of two turbines is almost the same, except of the equivalent onset velocity for downstream turbine, because its sweeping area may not be totally exposed to the wake effect of the upstream turbine. As figure 27 shows, when the two turbines are partly offset, similarly, a slightly decreased Ct benefits the total power output for 2 turbines when the onset wind speed is below rated speed 15 m/s. The curve of C_T is already smooth except for the

point where the wind speed is 14 m/s, in real practice, the C_T at that point will be altered to 0.55 to make the curve smoother.

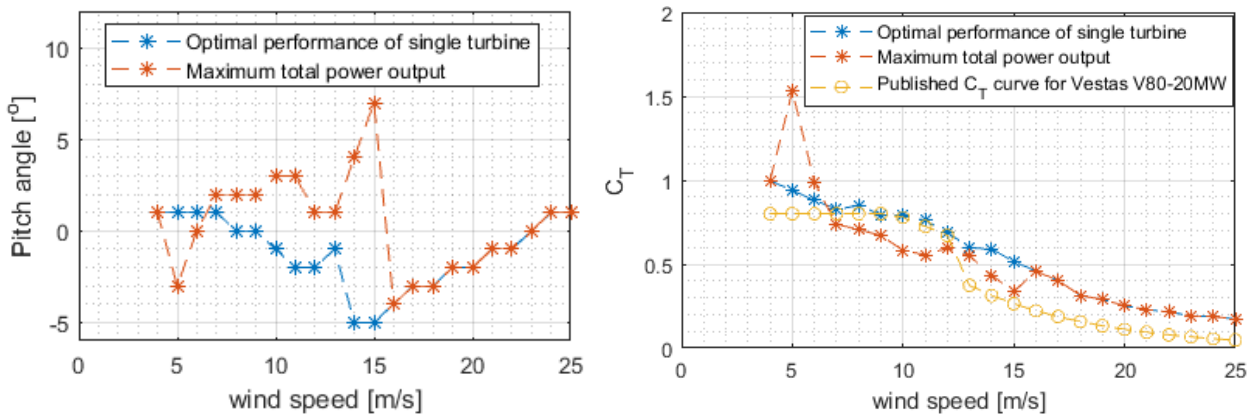

Fig. 26 Pitch angle comparison and C_T comparison under different operation strategies_inline

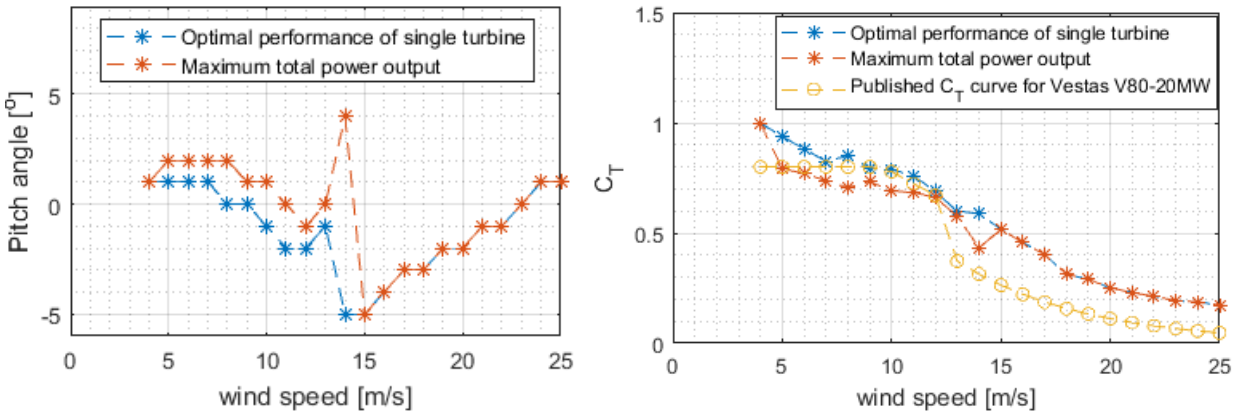

Fig. 27 Pitch angle comparison and C_T comparison under different operation strategies_partly-offset

When the two turbines are inline, the total power output difference is relatively obvious than the partly offset situation, as figure 28 shows. The red line under adjusted C_T of upstream turbine is slightly higher than the blue line when both of turbines are in optimal performance.

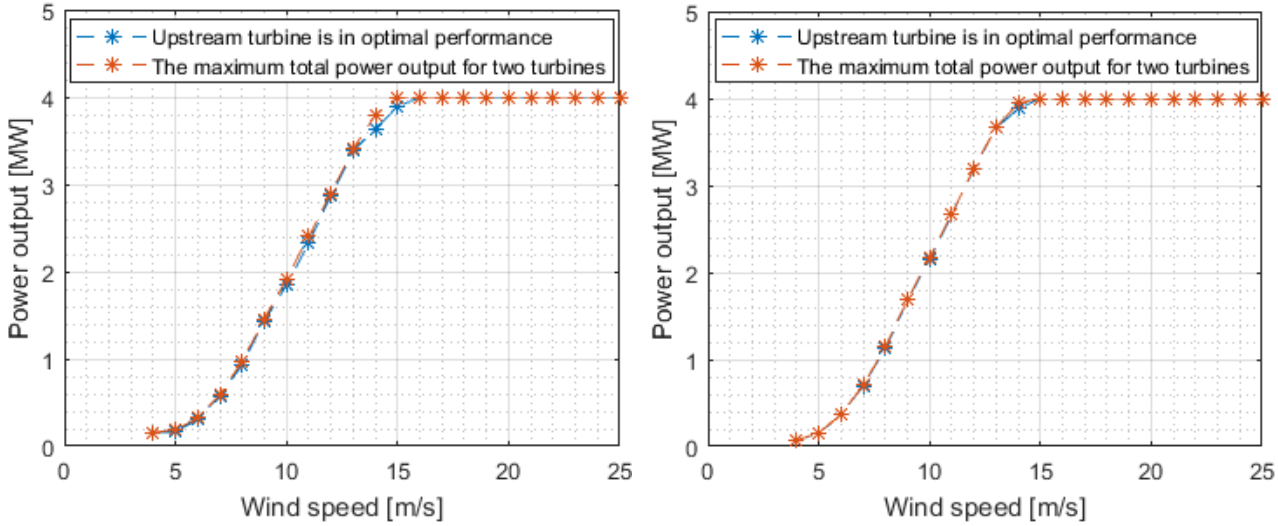

Fig. 28 Total power output in inline and partly-offset situations under 2 operation strategies

Reading the power output difference from the table 3 is easier since the difference between power output of 2 operation strategies is too small to be distinguished in the power curve according to time over 8760 hours in the next chapter.

Table 3 Power output difference in partly-offset under 2 operation strategies

Total power output [MW]												
Wind speed [m/s]	4	5	6	7	8	9	10	11	12	13	14	15
Optimal	0.070	0.153	0.362	0.697	1.121	1.680	2.147	2.662	3.196	3.660	3.884	4.000
Adjusted Ct	0.072	0.154	0.369	0.702	1.142	1.687	2.172	2.676	3.199	3.669	3.946	4.000
Power change	0.002	0.001	0.007	0.005	0.021	0.007	0.025	0.014	0.003	0.008	0.061	0.000
Power output of upstream turbine [MW]												
Optimal	0.005	0.111	0.262	0.465	0.723	1.049	1.276	1.526	1.774	1.963	2.000	2.000
Adjusted Ct	0.005	0.109	0.256	0.452	0.698	1.033	1.253	1.501	1.763	1.962	2.000	2.000
Power change	0.000	-0.002	-0.006	-0.013	-0.025	-0.016	-0.022	-0.026	-0.011	-0.001	0.000	0.000
Power output of downstream turbine [MW]												
Optimal	0.065	0.042	0.100	0.231	0.399	0.631	0.872	1.136	1.422	1.697	1.884	2.000
Adjusted Ct	0.067	0.045	0.112	0.250	0.444	0.654	0.919	1.175	1.436	1.707	1.946	2.000
Power increment	0.002	0.003	0.012	0.019	0.046	0.023	0.047	0.040	0.014	0.010	0.061	0.000

5 Impact of Pitch Control on Time-variation of Turbine Array Power Production

According to the above research, it can be guessed that the operation strategy using adjusted C_T will have a positive impact on wind power generation. This chapter will examine how these two operation strategies will affect the energy yield and power stability of actual wind farms. The smallest scale array is used as the research object, using the real wind data and the research methods in the previous sections.

5.1 Resource data

Before this section, no real wind data has been considered, an ideally uniform onset wind velocity is set for the upstream wind turbine and following background wind velocity (outside the wake). In real situation, the wind speed distribution in a certain space is not uniform, resulting in uneven force on the airfoil of the wind turbines. The wind gradient in vertical wind-profiles is very important that must be considered when designing a wind turbine structure to make sure its safe operation and work.

For wind turbine engineering, the variation of mean wind speed with height can be represented by an expression in this form (Heier & Waddington, 1998):

$$\frac{\overline{U}(z)}{\overline{U}(h)} = (\frac{z}{h})^{\alpha}; \quad (27)$$

Where $\overline{U}(z)$ is the velocity of wind (m/s) at height z, $\overline{U}(h)$ is the reference wind speed (m/s) at height 10m; α equals to 0.16 (or 1/7) typically for specific location that " neutral air above flat open coast (compatible with the environment where wind speed data has been collected)", known as Hellman's exponent (Martin Kaltschmitt, Wolfgang Streicher, 2007). Because the hub height and rotor diameter are fixed for the reference turbine, so onset wind velocity at any point at the rotor sweeping area can be calculated, then the equivalent velocity can be estimated by integral calculation. Assuming that the speed of wind is always perpendicular to the plane of the rotor's rotation, the equivalent onset wind U_0 speed equals to 1.3404 times U_{10} (reference wind speed at a height of 10m) approximately.

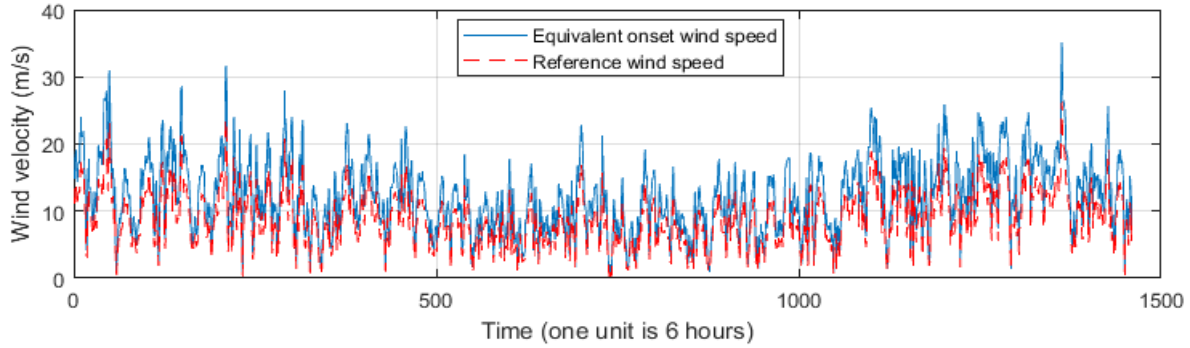

Fig. 29 Reference wind speed data and equivalent U0 for the wind turbine array

The wind data is composed by u and v components, should be primarily westerly winds, as figure 30 shows. This wind speed was collected at the point with latitude = 58.656998 and longitude = -3.122078. U and v refer to the velocity components in (when looking at it two-dimensionally) +x and +y (i.e. east and north) direction. Data source for this is European Centre for Medium Range Weather Forecasts (ECMRWF)-European Reanalysis (ERA) with a time step of 6 hours at a height of 10 m. The wind data of one-year (8760 hours) is as figure () shows, only the range of equivalent onset wind velocity from 4 to 25 m/s will used in the next simulation.

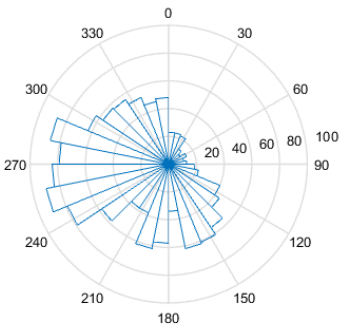

Fig. 30 Wind rose diagram

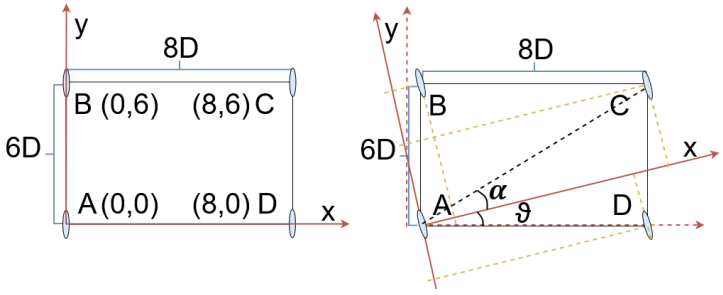

Fig. 31 Coordinate system of 4-turbine array unit

5.2 Maximum Power Output for 4-Turbines Array Unit

As figure 31 shows, the four reference turbines (A, B, C, D) are placed on the four vertices of the rectangle and the length and width of the rectangle are 8D and 6D. The four turbines will yaw as the wind direction changes so that the rotor plane is perpendicular to the wind heading (N. S. Moskalenko, Member, Rudion, Styczynski, & Wake, 2011). The direction of the X-axis coordinates is determined by the direction of U_0, and this defines the relative coordinates of three turbines' relative to turbine A which is at the origin (0, 0).

For example, in the case of figure 31, the onset wind for turbine A, B, D is U_0, only C or D may be affected by A, so only A (0, 0), C $(10\cos\alpha, 10\sin\alpha)$ and D $(8\cos\theta, -4\sin\theta)$ matter, in which θ and α can always be derived by u and v (east and north wind component respectively), will be influenced by 2 operation strategies. In conclusion, the number and position of interacting turbines are always determined by the wind direction. Refers to wind data and the reference turbine's C_T and C_P curves under pitch control, the power output simulation results are shown below.

First, for the two interacting turbines, the power output for the upstream turbine, downstream turbine and the total power output will be different when adopting different operation strategies. But the difference won't be very obvious, because the equivalent wind speed exceeds 15 m/s frequently since the data is from an offshore wind farm. When wind speed exceeds 15 m/s, there is no difference adopting the optimal power performance C_T curve of upstream turbine or alter the C_T. Two operation strategies can both achieve the maximum power output, satisfied by a variety of C_T of upstream turbine.

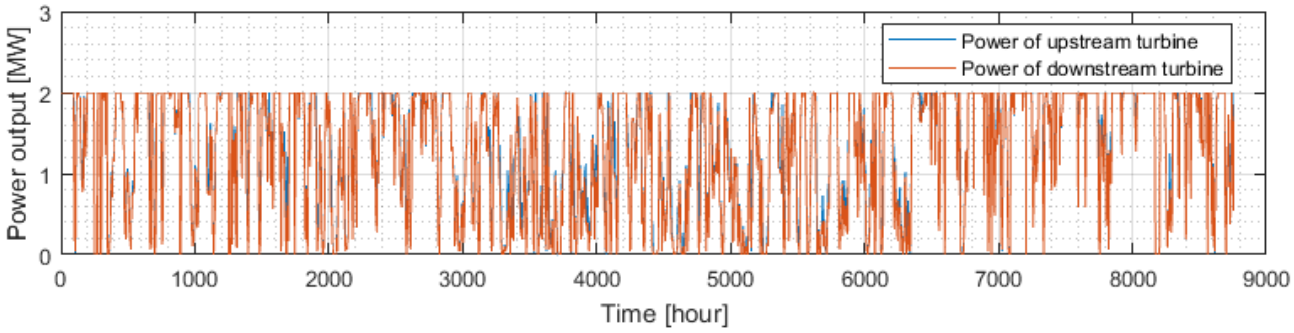

Fig. 32 Power history curve of two interacting wind turbines_optimal power performance

If the downstream turbine is exposed to the wake of the upstream turbine, the power output of the downstream turbine is always lower than the output of the upstream turbine because of the velocity deficit caused by the wake. This is why the blue line is higher than the red line when two turbines are interacting and wind speed is lower than rated speed in figure 31. The difference of power output between the two turbines can reach 0.76 MW when the optimal performance operation strategy is applied.

The difference of power output between the two turbines can be effectively decreased when the adjusted C_T operation strategy is applied. As figure 33 shows, the maximum power output difference is only 0.53 MW for the second operation strategy, with a higher value of the total power output.

There are only 15.137% (221) of time points that satisfy the two statistical requirements: $4 \leq U_0 \leq 15\ m/s$ and the downstream turbine should be exposed to the wake area of upstream turbine, which means only in these 1326 (221×6) hours, the total output is different under two operation strategies. These 1326 hours are the critical time to make the adjusted C_T meaningful for increasing the total power output.

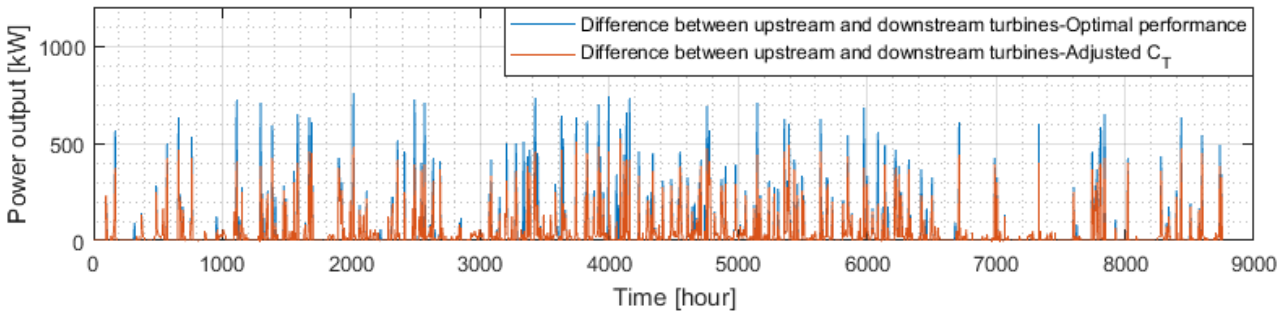

Fig. 33 Power output difference between upstream and downstream turbines

Even there is a difference of the total power output for the two interacting turbines, it is still too vague to be observed from the figure. Difference is more obvious from the power data of a representative sampling time point. As table 5 shows, the energy yield will increase by 199.024 kWh for the 6 hours (from 6222h to 6228h) if adjusted C_T is adopted for the upstream turbine, in which case the turbine C will affect turbine A and the U_0 equals to 8.226 m/s.

Table 4 Power data of a sampling time point

No. of sampling	1037
Time point [h]	6222
U_East_X axis	-3.556
V_North_Y axis	-5.002
U_10m	6.137
U_equivalent onset	8.226
Total power output [MW]	
Optimal	1.118
Adjusted Ct	1.151
Power change	0.033
Power output of upstream turbine [MW]	
Optimal	0.792
Adjusted Ct	0.761
Power change	-0.031
Power output of downstream turbine [MW]	
Optimal	0.326
Adjusted Ct	0.390
Power change	0.064
Energy yield for 6 hours [kWh]	
Optimal	6705.848
Adjusted Ct	6904.871
Energy increment	199.024

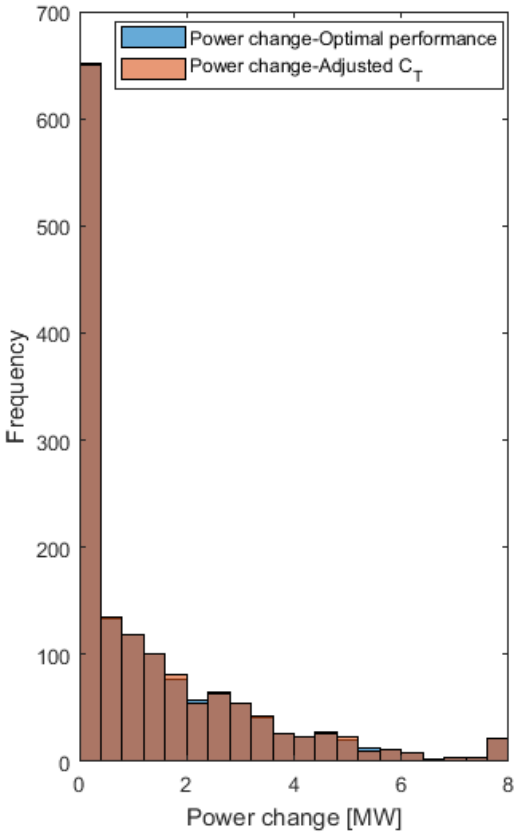

Fig. 34 Time rate of change of the total power

The other attribute of the second operation strategy is that it can make the total power output more stable. The rate of total power change (absolute value that it can be increment or decrement) for interval 1.6MW to 2MW and 4.8MW to 5.2MW will increase if the second operation strategy is applied, although the difference is not signficant, still improving the stability of total power output for this array, as figure 34 shows.

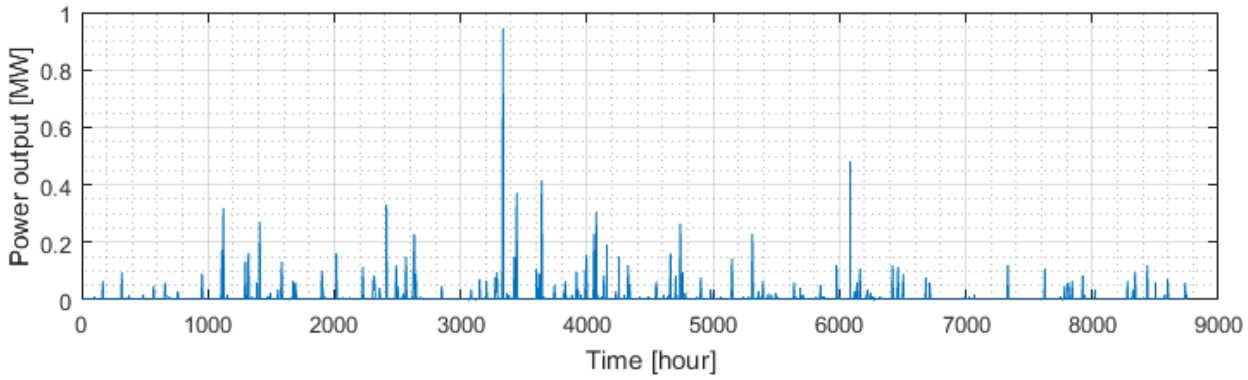

Fig. 35 Total power output difference of the four turbines under two operation strategies

As figure 34 shows, the total power output difference of the four turbines under two operation strategies can reach 0.95MW. As table () shows, by adopting adjusted C_T operation strategy, the total energy yield of upstream turbine (can be any one or two of these four turbines, depending on the direction of U_0) will decreases by 52.2 MWh. To the opposite, the total energy yield of downstream turbine will increase by 128.4 MWh. As a result, by using adjusted C_T value, the total energy yield for the year will increase by 76.2 MWh, which is very promising.

The energy yield increment is not very high compared to the total energy yield for three reasons: the reference turbine's rated power is only 2 MW; only on very limited condition of wind speed and direction, the adjusted C_T will make sense for total power output; the scale of the research array is very small. Therefore, the second strategy is still very valuable and indicates higher increment for real wind farms of large scale.

Table 5 The energy yield of the 4-turbines array unit for a year

Energy yield [MWh]	Turbine 1	Turbine 2	Turbine 3	Turbine 4	Total
Optimal	11790.6	11330.4	11775.6	11478.6	46375.2
Adjusted Ct	11760	11406	11754	11531.4	46451.4
Energy change [MWh]	-30.6	75.6	-21.6	52.8	76.2

6 Conclusion and Recommendation

In this thesis, the power output for a four-turbines array unit was successfully simulated to test the impact of pitch control on time-variation of turbine array power production, using the Larsen wake model, real wind data and basic geometric knowledge. Two operation strategies: using the C_T to make both turbines work in their optimal power performance or adjusting the C_T of the upstream turbine to a lower value to increase the total power output, were applied in the power output simulation and evaluated from two aspects: total energy yield and stability of total power output. The summary of the main conclusions is as follows:

The energy yield of a 4-turbines array unit has been calculated according to real wind data for a year. It is proved that using the adjusted C_T operation strategy can increase the energy yield by 76.2 MW for the array, which only accounts for only 0.164% of the total energy yield since there are a lot of constraints that blunt the advantages of adjusting C_T. It can be guessed that the strategy of increasing total energy yield by adjusting C_T is more effective in large-scale wind farms

with relatively lower but stable wind speed. In addition, the adjusted C_T operation strategy can also slightly improve the stability of total power output for this array.

The simulation in the last chapter is based on Larsen wake model. Because the Larsen model was chosen as the most appropriate one for further simulation by evaluating the four analytical wake models rely on comparison with standard CFD simulation result for single wake. The Larsen model can better reflect the law that velocity deficit decreases as radial distance increases, which means the velocity in the center of wake is always the lowest. The velocity distribution of Larsen model is closest to the CFD simulation result as shown in transverse profiles. Although the wake expansion rate in Larsen simulation is much lower than in CFD simulation, there is little influence in further power output simulation since in CFD simulation the wind normalized speed is almost 1 outside the area above Larsen wake diameter. Three wake combination methods also have been evaluated, although were not used for the final power output simulation. The Linear method that add the velocity deficit generated by each wake in the area where different wakes are superimposed is the most accurate way to combine wake field.

For a set of reference turbines, only a particular C_T of the upstream turbine can satisfy the maximum total power output for the two turbines, which is slightly lower than the optimal performance C_T curve for a single turbine when the U_0 is lower than rated speed. In this situation, using the adjusted C_T operation strategy is meaningful and the effect is more significant when the downstream turbine is totally exposed to the wake area of the upstream turbine.

A variety of pitch angle can meet the highest total power output requirement when the onset wind speed U_0 is very high that close to the cut-out wind speed. And there is no difference adopting either of the two operation strategies.

In this MSc dissertation project, only the simplest array types have been tested under two different operation strategies in the last two chapters. However, the real wind farms are large in scale, having much more turbines, in which the interacting effect between turbines are also much more complicated. In other words, using the adjusted C_T may benefit the total power output more for a real offshore wind farm, even according to the same wind data. Because the chance that upstream turbine's wake influences downstream turbines will increase a lot as the scale of the array increases. In addition, the superposition of different wakes will induce higher velocity deficit.

It is recommended to do further power output and energy yield simulation for a real wind farm with more complex layout to establish whether pitch control could be exploited for power smoothing or for load smoothing.

Other methods of controlling the time varying power output or loading could also be investigated by a wind farm developer like the design of turbine spacing, combination of turbines of different power output in a wind farm, arrangement (layout) of wind turbines etc.

Reference

[1] Agency, I. E. (2016). World Energy Outlook 2016, Special Focus on Renewable Energy. *International Ene*, 395–543. https://doi.org/10.1787/weo-2004-en

[2] Archer, C. L., Vasel-Be-Hagh, A., Yan, C., Wu, S., Pan, Y., Brodie, J. F., & Maguire, A. E. (2018). Review and evaluation of wake loss models for wind energy applications. *Applied Energy*, *226*(July), 1187–1207. https://doi.org/10.1016/j.apenergy.2018.05.085

[3] B.Sanderse, S. P. va. der P. (2011). Review of computational fluid dynamics for wind turbine wake aerodynamics. *Wind Energy*, *14*, 799–819. https://doi.org/10.1002/we.458

[4] Barthebnie, R., Larsen, G., Pryor, S., Jørgensen, H., Bergström, H., Schlez, W., … Magnusson, M. (2004). ENDOW (Efficient Development of Offshore Wind Farms): Modelling wake and boundary layer interactions. *Wind Energy*, *7*(3), 225–245. https://doi.org/10.1002/we.121

[5] Choi, N. J., Hyun Nam, S., Hyun Jeong, J., & Chun Kim, K. (2013). Numerical study on the horizontal axis turbines arrangement in a wind farm: Effect of separation distance on the turbine aerodynamic power output. *Journal of Wind Engineering and Industrial Aerodynamics*, *117*, 11–17. https://doi.org/10.1016/j.jweia.2013.04.005

[6] Crasto, G., Gravdahl, A. R., Castellani, F., & Piccioni, E. (2012). Wake modeling with the actuator Disc concept. *Energy Procedia*, *24*(January), 385–392. https://doi.org/10.1016/j.egypro.2012.06.122

[7] Frandsen, S., Barthelmie, R., Pryor, S., Rathmann, O., & Larsen, S. (2006). Deficit in Large Offshore Wind Farms, (January), 39–53. https://doi.org/10.1002/we

[8] Global Wind Energy Council. (2017). Global Wind Energy Outlook 2016. *Global Wind Energy Council*, (October), 1–60. Retrieved from http://files.gwec.net/register?file=/files/GlobalWindEnergyOutlook2016

[9] González-Longatt, F., Wall, P. P., & Terzija, V. (2012). Wake effect in wind farm performance: Steady-state and dynamic behavior. *Renewable Energy*, *39*(1), 329–338. https://doi.org/10.1016/j.renene.2011.08.053

[10] Gunn, K., Stock-Williams, C., Burke, M., Willden, R., Vogel, C., Hunter, W., … Schmidt, S. R. (2016). Limitations to the validity of single wake superposition in wind farm yield assessment.

Journal of Physics: Conference Series, *749*(1). https://doi.org/10.1088/1742-6596/749/1/012003

[11] Heier, S., & Waddington, R. (1998). *Grid integration of wind energy conversion systems*.

[12] Ishihara, T., Yamaguchi, a., & Fujino, Y. (2004). Development of a new wake model based on a wind tunnel experiment. *Global Wind Power*, 6. Retrieved from http://windeng.t.u-tokyo.ac.jp/ishihara/posters/2004_gwp_poster.pdf%5Cnhttp://windeng.t.u-tokyo.ac.jp/ishihara/proceedings/2004-5_poster.pdf

[13] Jensen, N. O. (1983). A note on wind generator interaction. *Risø-M-2411 Risø National Laboratory Roskilde*, 1–16. https://doi.org/Riso-M-2411

[14] Kollwitz, J. (2016). Defining the Wake Decay Constant As a Function of Turbulence Intensity To Model Wake Losses in Onshore Wind Farms. Retrieved from http://www.diva-portal.org/smash/get/diva2:1044398/FULLTEXT01.pdf

[15] Martin Kaltschmitt, Wolfgang Streicher, A. W. (2007). *Renewable Energy: Technology, Economics, and Envioronment*. Springer.

[16] Miao, W., Li, C., Pavesi, G., Yang, J., & Xie, X. (2017). Investigation of wake characteristics of a yawed HAWT and its impacts on the inline downstream wind turbine using unsteady CFD. *Journal of Wind Engineering and Industrial Aerodynamics*, *168*(December 2015), 60–71. https://doi.org/10.1016/j.jweia.2017.05.002

[17] Moskalenko, N., Rudion, K., & Orths, A. (2010a). Study of wake effects for offshore wind farm planning. *2010 Modern Electric Power Systems*, 1–7.

[18] Moskalenko, N., Rudion, K., & Orths, A. (2010b). Study of wake effects for offshore wind farm planning. *2010 Modern Electric Power Systems*, (January 2015), 1–7.

[19] Moskalenko, N. S., Member, S., Rudion, K., Styczynski, Z. A., & Wake, A. (2011). Yaw Angle Pattern (OYAP), 1–6.

[20] Müller, S., Deicke, M., & W., & Rik Doncker, D. (2002). Doubly fed induction generator systems for wind turbines. *Industry Applications Magazine, IEEE*, *8*(3), 26–33. https://doi.org/10.1109/2943.999610

[21] Son, E., Lee, S., Hwang, B., & Lee, S. (2014). Characteristics of turbine spacing in a wind farm using an optimal design process. *Renewable Energy*, *65*, 245–249. https://doi.org/10.1016/j.renene.2013.09.022

[22] Sun, H., & Yang, H. (2018a). Study on an innovative three-dimensional wind turbine wake model. *Applied Energy*, *226*(March), 483–493. https://doi.org/10.1016/j.apenergy.2018.06.027

[23] Sun, H., & Yang, H. (2018b). Study on three wake models' effect on wind energy estimation in Hong Kong. *Energy Procedia*, *145*, 271–276. https://doi.org/10.1016/j.egypro.2018.04.050

[24] Takahashi, R., Ichita, H., Tamura, J., Kimura, M., Ichinose, M., Futami, M. O., & Ide, K. (2010). Efficiency calculation of wind turbine generation system with doubly-fed induction generator. *19th International Conference on Electrical Machines, ICEM 2010*, 4–7. https://doi.org/10.1109/ICELMACH.2010.5608319

[25] Tian, L., Zhu, W., Shen, W., Song, Y., & Zhao, N. (2017). Prediction of multi-wake problems using an improved Jensen wake model. *Renewable Energy*, *102*, 457–469. https://doi.org/10.1016/j.renene.2016.10.065

[26] Tong, W., Chowdhury, S., Zhang, J., & Messac, A. (2012). Impact of Different Wake Models On the Estimation of Wind Farm Power Generation. *12th AIAA Aviation Technology, Integration, and Operations (ATIO) Conference and 14th AIAA/ISSM*, (September), 1–13. https://doi.org/10.2514/6.2012-5430

[27] Vestas. (2011). V80-2.0MW Technical Catalogue. *Www.Vestas.Com*, 1–20.

Appendix 1: Project Schedule

Project activity	Week											
	1	2	3	4	5	6	7	8	9	10	11	12
Literature review												
Summary of 4 analytical wake models												
Summary of 3 wake combination methods												
MATLAB program of single wake												
Evaluation of 4 analytical wake models												
MATLAB program of wake superposition												
Evaluation of 3 wake combination methods												
Research of the reference turbine												
Power output simulation for 2 turbines array												
Collection and analysis of wind data												
Power output and energy yield simulation												
for 4 turbines array under 2 different												
operation strategies												
Write the thesis draft according to work												
process and results mentioned above												
Ask advice from my supervisor												
Thesis draft review and improvement												
Submit dissertation												

Appendix 2: Risk Assessment

Date: 17/06/2018	Assessed by: Fengnan Sun	Checked / Validated* by: Dr. Timothy Stallard	Location: Barnes Wallis Computer Cluster	Assessment ref no	Review date: 31/08/2018
Task / premises: MSc dissertation project based on MATLAB programming.					

Activity	Hazard	Who might be harmed and how	Existing measures to control risk	Risk rating	Result
Mental Stress	Health problem	Fengnan Sun Work stress can induce psychological problems.	Make a good plan of the dissertation project. Get advice from personal tutor or supervisor. Communicate with friends.	Low	
Use of printer	Toner inhalation	Fengnan Sun Improper operation or damaged machine.	Che the printer before using, follow by instructions.	Low	
Working in front of comput er	Back pain, neck-ache, and visual fatigue	Fengnan Sun Long time working in front of the computer or wrong sitting posture.	Adjust chair position and computer screen as suggested. Exercise every day.	Medium	